Tripod Ligands Containing a Mixed P/N/S Donor Set: Synthesis and Coordination Chemistry

Albrecht Jacobi, Gottfried Huttner*, and Ute Winterhalter

Anorganisch-Chemisches Institut der Universität Heidelberg,
Im Neuenheimer Feld 270, D-69120 Heidelberg, Germany

Received May 12, 1997

Keywords: Tripodal ligands / Aminolytic cleavage of oxetanes / Tripod molybdenum compounds / Mixed donor set ligands

The preparation of neopentane-based tripod ligands $CH_3C(CH_2X)(CH_2Y)(CH_2Z)$ **3** (X = NR_2, NHR; Y = PR_2; Z = PR_2, SR, S^-) in a convergent manner is described. The procedure is based on the aminolytic cleavage of functionalized oxetanes $CH_3C(CH_2OCH_2)CH_2R$ **1** by primary or secondary amines, leading to functionalized amino alcohols $CH_3C(CH_2NHR')(CH_2OH)(CH_2R)$ or $CH_3C(CH_2NR'_2)$-$(CH_2OH)(CH_2R)$ **2**. The appropriate activation of the R (e.g. OR) and OH groups present in **2** allows for substitution vs. SR or PR_2 donor functions. Depending on the nature of the groups present in each reaction step, various protection and deprotection steps have to be taken in the course of this type of preparation of the tripod ligands **3**. By reaction with $(CH_3CN)_3Mo(CO)_3$, ligands **3** form $Mo(CO)_4$ derivatives **4** or $Mo(CO)_3$ derivatives **5**, depending on the reaction conditions. In compounds **4**, the ligands are coordinated in a bidentate mode with the soft donor atoms (P, S) coordinated and the hard donor function playing the role of the dangling arm. In the trihapto bonding mode present in **5**, all three donor functions, two soft (P, S) and one hard (NHR', NR'_2), are coordinated. The two types of coordination compounds may be interconverted: **4e** (X = NMe_2, Y = PPh_2, Z = S*i*Pr) with a non-coordinating CH_2NMe_2 group is transformed into **5c** upon photolytic decarbonylation. Under 1 bar CO at 20°C, **5c** reverts to **4e**. X-ray structure analysis of a series of compounds of types **4** and **5** reveals characteristics of the relevant conformational patterns. All compounds have been fully characterized by the standard analytical techniques (NMR, MS), as well as elemental analysis.

Introduction

The neopentane backbone in tripod ligands of the type $CH_3C(CH_2X)(CH_2Y)(CH_2Z)$, (X, Y, Z = donor groups) provides an ideal spacer to allow for the facial coordination of such ligands to a broad variety of electropositive elements[1][2]. When these ligands are coordinated to form tripod metal templates, tripod–M, they effectively block one half of the coordination sphere around the metal. At the same time, the individual shape of the donor groups and the substituents will shape the remaining part of the coordination space in a specific and predictable way[3]. The capability of tripod ligands to form a kind of sterically protected reaction pocket in their templates, tripod–M, may be seen as the underlying reason for the fact that many quite unconventional ML_n fragments have been stabilized as their tripod derivatives tripod–ML_n[2].

To date, the potential that neopentane-based tripod ligands thus appear to have in coordination chemistry[1][2] has only scarcely been exploited in catalysis[4]. The additional potential lying in the possibility of deliberately varying the kind of donor groups fixed to the neopentane framework is also only marginally developed. While tripod ligands of constitutional C_3 symmetry with three equal donor groups are readily accessible and have been extensively used in the field, such ligands with constitutional C_s or C_1 symmetry, having up to three different phosphorus donors, have only recently been described[5]. Nevertheless, even enantioselective syntheses of ligands of this type containing three different phosphorus donors have been designed[6]. Problems in synthesizing such ligands are general problems associated with neopentane chemistry (sluggish S_N2-reactivity, rearrangements)[5c][7][8a], which in this context are further enhanced by problems pertinent to the chemistry of multifunctional compounds. These problems have largely been overcome in the case where all of the donor groups have phosphorus donor centers[5][6]. For sulfur donors, the problems have in part been solved as well[5b][5c][5d][5e][5f][5g][9], while mixed donor set tripod ligands incorporating nitrogen-centered donors are not yet generally accessible[8]. It is the purpose of this paper to present synthetic procedures of a more general scope, which allow the preparation of $CH_3C(CH_2X)(CH_2Y)(CH_2Z)$ ligands, X, Y being sulfur and phosphorus donors and Z being an NR_2 or NHR group. Coordination capabilities of these ligands containing up to three different donor atoms (P, S, N) are demonstrated by the synthesis and structural characterization of a series of $Mo(CO)_4$ and $Mo(CO)_3$ derivatives.

Ligand Synthesis

The different strategies so far developed for the synthesis of neopentane-based tripod ligands $CH_3C(CH_2X)(CH_2Y)$-(CH_2Z) generally involve the introduction of the donor functions as nucleophiles to substitute some nucleophugic

  0009–2940/97/0909–1279 $ 17.50+.50/0

substituents at the neopentane scaffolding. While this procedure works well with O, S, and P donors, the introduction of N donors using this type of approach is limited by the lack of appropriate nitrogen-centered nucleophiles. The standard procedure of using N_3^- as the nitrogen nucleophile is only applicable as long as there is no phosphane substituent in the molecule; otherwise introduction of the azide substituent is invariably accompanied by an immediate intramolecular Staudinger reaction (oxidation of P^{III} to P^V). Potassium phthalimide has been shown to substitute neopentane-based tosylate groups[10] and might be an alternative, even though the reactivity of neopentane systems bearing large substituents such as PPh_2 is possibly too low to allow this variant to proceed successfully. It is desirable that the introduction of the nitrogen donor function is convergent, in the sense that it is the first donor function introduced into a starting compound that has already been shown to allow the synthesis of a whole range of mixed donor set tripod ligands with various O, S, and P donors. Well-behaved starting compounds in this sense are functionalized oxetanes (Scheme 1), which have been used to construct a whole plethora of mixed donor set neopentane-based tripod ligands[5c][5f][5h][5i][8c].

Scheme 1. Oxetanes as precursors for tripod ligands

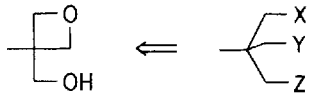

Two strategies are available for eliciting the reactivity inherent in the oxetane ring: Electrophilic ring-opening by reagents such as HBr leads to one CH_2Br and one CH_2OH group, after which the CH_2OH group may be electrophilically activated in the next reaction step[11]. Alternatively, nucleophilic ring-opening of the oxetane by PR_2^- nucleophiles incorporates a PR_2 group and generates a CH_2OH group at the same time[5h]. Electrophilic activation of the OH group is then possible as the next reaction step, with the PR_2 group protected as a phosphanoborane[5h]. This second approach is especially appealing because it introduces the desired donor group and generates a precursor to further nucleophilic substitution in a single step. It would therefore be desirable to find conditions under which NR_2 or NHR groups would nucleophilically open the oxetane. Such conditions have in fact been described for some specific oxetanes and some specific amine nucleophiles[11]. It was necessary to ascertain whether this approach would be feasible with appropriately substituted oxetanes and, moreover, to evaluate its generality with respect to other donor groups already introduced. Once this key question has been answered, the standard procedures that have already been developed for the introduction of PR_2 and SR entities[5f][5h][9] and variations thereof should facilitate the preparation of an almost unrestricted range of tripod products.

To develop this idea, a number of oxetanes of type **1** have been prepared following published procedures or suitably modified adaptations thereof (Scheme 2).

Scheme 2. Functionalized oxetanes for tripod synthesis

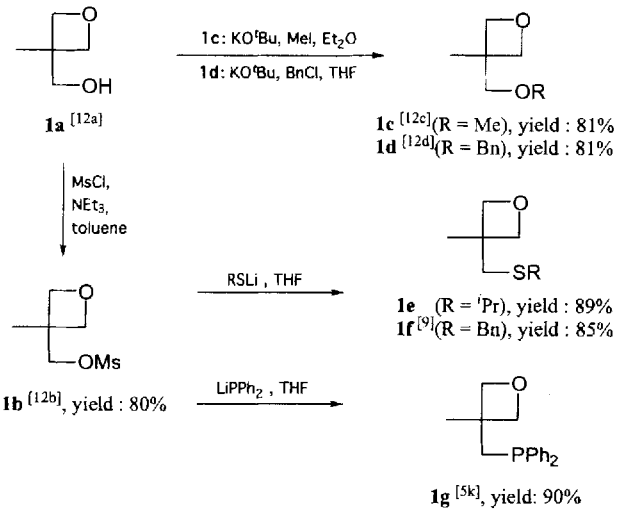

The compounds were obtained as colourless oils after purification by distillation, giving correct elemental analyses and mass spectra (see Experimental Section). The constitution of **1e** and **1f** as given (Scheme 2) is unequivocally substantiated by the relevant NMR data (Table 1).

Table 1. ^{1}H- and ^{13}C-NMR spectra (solvent $CDCl_3$) of **1e**, **1f**

	^{1}H NMR [δ values]	^{13}C NMR [δ values]
1e	1.21 [d, 6 H, $^3J_{HH}$ = 6.6 Hz, $CH(CH_3)$], 1.27 (s, 3 H, $CqCH_3$), 2.80 (s, 2 H, CH_2S), 2.84 [sept, 1 H, $^3J_{HH}$ = 6.6 Hz, $CH(CH_3)$], 4.33, 4.38 (2d, 4 H, $^2J_{HH}$ = 5.8 Hz, oxetane-CH_2).	22.9 (s, $CqCH_3$), 23.2 [s, $CH(CH_3)$], 35.9 [s, $CH(CH_3)$], 39.7 (s, CH_2S), 41.5 (s, *Cq*), 81.7 (s, oxetane-CH_2).
1f	1.36 (s, 3 H, $CqCH_3$), 2.78 (s, 2 H, CH_2S), 3.76 (s, 2 H, CH_2Ph), 4.34, 4.41 (2d, 4 H, $^2J_{HH}$ = 5.9 Hz, oxetane-CH_2), 7.26–7.36 (m, 5 H, arom. H).	23.0 (s, $CqCH_3$), 37.5 (s, CH_2Ph), 39.7 (s, *Cq*), 40.8 (s, CH_2S), 81.7 (s, oxetane-CH_2), 126.9–138.0 (*arom. C*).

The presence of an oxetane ring is in each case clearly evident from the characteristic ^{1}H-NMR signals with a geminal HH-coupling between the diastereotopic methylene protons of around 6 Hz (Table 1)[5h]. The ^{13}C chemical shift of the methylene carbon atoms (Table 1) of the oxetane ring is again characteristic of this type of four-membered cycle[5h].

The nucleophilic opening of the oxetane ring in **1a** with $HNMe_2/H_2O$ as the nitrogen nucleophile has been reported in the literature to occur after prolonged heating at a pressure of around 30 bar[11]. A few other secondary amines have been found to be effective in this type of reaction, whereas attempts to use ammonia as the nucleophile were unsuccessful[11]. Compound **2a** was prepared from **1a** following this procedure. On the basis of the ^{1}H-NMR spectra, the reaction was found to proceed almost quantita-

tively. After purification of the crude product by distillation, yields of around 70% were obtained (Scheme 3).

Scheme 3. Aminolytic cleavage of oxctanes

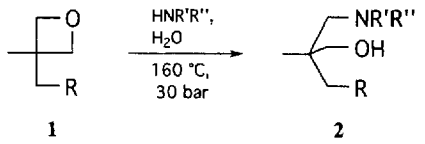

1 **2**

	R	NR'R''	reaction time [h]	yield [%][a]
2a	OH	NMe_2	20	70[b]
2b	OH	NMeH	24	86
2c	OH	NBnH	48	52
2d	OBn	NMe_2	96	85
2e	OBn	NMeH	84	69
2f	S*i*Pr	NMe_2	60	76
2g	SBn	NMe_2	120	54
–	PPh_2	NMe_2	168	–

[a] Analytically pure product after distillation through a 20 cm Vigreux column. – [b] For comparison see ref.[11].

While this type of reaction has not previously been reported for primary amines as nucleophiles, it was found that under appropriate conditions methylamine H_2NMe and benzylamine H_2NBn react accordingly to produce **2b** and **2c**, respectively. The tolerability of other groups in place of the OH group of **1a** was checked by using **1d**–**1g** as the starting compounds. **1d** reacts with $HNMe_2$ to produce **2d** and with H_2NMe to produce **2e** in fair yields. The reaction times needed are longer than those required with **1a** as the starting compound (Scheme 3). Both **1e** and **1f** were reacted with $HNMe_2$ as the nucleophile. Prolonged heating produced **2f** and **2g** in acceptable yields (Scheme 3). With **1g** as the starting compound, none of the amine nucleophiles found to be effective when starting from **1a**, **1d**, **1e**, **1f** produced any useful amount of ring-opened product. A change of the solvent mixture (H_2O/THF, EtOH) did not lead to any improvement, nor did a change of the reaction temperature or time. The result of this series of experiments was either no reaction or decomposition of the starting compound to an ill-defined mixture of products.

Compounds **2a**–**2g** were obtained as analytically pure colourless oils after distillation of the crude products, in yields as given in Scheme 3. The connectivity as shown in Scheme 3 is in accord with the NMR data of **2a**–**2g** (Table 2).

The three CH_2 groups appear in clearly separated ranges depending on whether the substituent atom is O, N, or S (Table 2). For **2a**–**2c**, which contain two CH_2OH groups, the CH_2 protons are nevertheless diastereotopic. This diastereotopicity is only indicated for **2a** and **2b** by relatively broad signals, while for **2c** a multiplet structure is apparent (Table 2). For the chiral, racemic products **2d**–**2g**, the three different CH_2 groups show the appropriate geminal coupling with characteristic coupling constants in almost all cases (Table 2). ^{13}C resonances of **2a**–**2g** correspond in the number as well as in the type (135°-DEPT) of the signals to the proposed structure (Table 2).

Table 2. ^1H- and ^{13}C-NMR spectra (solvent $CDCl_3$) of **2a**–**2l**

	^1H NMR [δ values]	^{13}C NMR [δ values]
2a	0.72 (s, 3 H, CqCH_3), 2.24 (s, 6 H, NMe_2), 2.40 (s, 2 H, CH_2N), 3.54 (br. s, 4 H, CH_2OH).	ref.[11]
2b	0.74 (s, 3 H, CqCH_3), 2.39 (s, 3 H, N*Me*), 2.73 (s, 2 H, CH_2N), 3.66 (br. s, 4 H, CH_2OH).	18.6 (s, CqCH_3), 36.9 (s, N*Me*), 39.1 (s, *Cq*), 60.3 (s, CH_2N), 70.1 (s, CH_2OH).
2c	0.72 (s, 3 H, CqCH_3), 2.83 (s, 2 H, CH_2N), 3.70 (m, 4 H, CH_2OH), 3.77 (s, 2 H, CH_2Ph), 7.25–7.35 (m, 5 H, *arom. H*).	18.7 (s, CqCH_3), 39.1 (s, *Cq*), 54.5, 57.7 (2s, CH_2N / CH_2Ph), 70.5 (s, CH_2OH), 127.0–139.1 (*arom. C*).
2d	0.88 (s, 3 H, CqCH_3), 2.31 (s, 6 H, NMe_2), 2.36, 2.69 (2d, 2 H, $^2J_{HH}$ = 13.7 Hz, CH_2N), 3.36, 3.54 (2d, 2 H, $^2J_{HH}$ = 9.0 Hz, CH_2OBn), 3.59, 3.66 (2d, 2 H, $^2J_{HH}$ = 10.4 Hz, CH_2OH), 4.52 (br. s, 2 H, CH_2Ph), 7.27–7.35 (m, 5 H, *arom. H*).	20.4 (s, CqCH_3), 40.2 (s, *Cq*), 48.6 (s, NMe_2), 67.2 (s, CH_2N), 71.4 (s, CH_2OH), 73.7, 75.0 (2s, CH_2OBn / CH_2Ph), 127.9–139.0 (*arom. C*).
2e	0.89 (s, 3 H, CqCH_3), 2.37 (s, 3 H, N*Me*), 2.52, 2.86 (2d, 2 H, $^2J_{HH}$ = 11.8 Hz, CH_2N), 3.32, 3.50 (2d, 2 H, $^2J_{HH}$ = 9.1 Hz, CH_2OBn), 3.55, 3.63 (2d, 2 H, $^2J_{HH}$ = 10.8 Hz, CH_2OH), 4.48, 4.56 (2d, 2 H, $^2J_{HH}$ = 12.3 Hz, CH_2Ph), 7.27–7.37 (m, 5 H, *arom. H*).	19.0 (s, CqCH$_3$), 36.9 (s, N*Me*), 39.1 (s, *Cq*), 58.9 (s, CH_2N), 70.8 (s, CH_2OH), 73.1, 74.3 (2s, CH_2OBn / CH_2Ph), 127.2–138.2 (*arom. C*).
2f	0.81 (s, 3 H, CqCH_3), 1.16 [d, 6 H, $^3J_{HH}$ = 6.2 Hz, CH(CH_3)], 2.23 (s, 6 H, NMe_2), 2.27, 2.50 (2d, 2 H, $^2J_{HH}$ = 13.8 Hz, CH_2N), 2.47, 2.63 (2d, 2 H, $^2J_{HH}$ = 12.5 Hz, CH_2S), 2.76 [sept, 1 H, $^3J_{HH}$ = 6.2 Hz, CH(CH$_3$)], 3.49 (s, 2 H, CH_2OH).	21.0 (s, CqCH$_3$), 23.2, 23.3 [2s, CH(CH$_3$)], 36.0 [s, CH(CH$_3$)], 37.7 (s, CH_2S), 38.8 (s, *Cq*), 47.9 (s, NMe_2), 68.3 (s, CH_2N), 71.7 (s, CH_2OH).
2g	0.90 (s, 3 H, CqCH_3), 2.30 (s, 6 H, NMe_2), 2.38, 2.57 (2d, 2 H, $^2J_{HH}$ = 13.8 Hz, CH_2N), 2.57, 2.61 (2d, 2 H, $^2J_{HH}$ = 12.5 Hz, CH_2S), 3.67 (s, 2 H, CH_2OH), 3.75 (s, 2 H, CH_2Ph), 7.25–7.37 (m, 5 H, arom. H).	21.7 (s, CqCH$_3$), 38.3, 39.4 (2s, CH_2S, CH_2Ph), 39.8 (s, *Cq*), 48.6 (s, NMe_2), 69.1 (s, CH_2N), 72.2 (s, CH_2OH), 127.4–138.9 (*arom. C*).
2h	0.78 (s, 3 H, CqCH_3), 1.42, 1.55, 2.54 (3m, 2 H, 4 H, 4 H, piperidine-CH_2), 2.46 (s, 2 H, CH_2N), 3.59, 3.67 (2d, 4 H, $^2J_{HH}$ = 11.0 Hz, CH_2OH).	19.2 (s, CqCH$_3$), 23.3, 26.2, 56.9 (3s, *piperidine-C*), 39.6 (s, *Cq*), 66.6 (s, CH_2N), 68.4 (s, CH_2OH).
2i	0.82 (s, 3 H, CqCH_3), 1.40, 1.55, 2.50 (3m, 2 H, 4 H, 4 H, piperidine-CH_2), 2.28, 2.62 (2d, 2 H, $^2J_{HH}$ = 14.2 Hz, CH_2N), 3.26, 3.39 (2d, 2 H, $^2J_{HH}$ = 9.1 Hz, CH_2OMe), 3.33 (s, 3 H, O*Me*), 3.54, 3.61 (2d, 2 H, $^2J_{HH}$ = 10.7 Hz, CH_2OH).	19.6 (s, CqCH$_3$), 23.4, 26.2, 56.8 (3s, *piperidine-C*), 39.2 (s, *Cq*), 58.9 (s, O*Me*), 65.9 (s, CH_2N), 70.6 (s, CH_2OH), 76.9 (s, CH_2OMe).
2j	0.96 (s, 3 H, CqCH_3), 1.47 (s, 9 H, *Boc*), 2.89 (s, 3 H, N*Me*), 3.20–3.36 (m, 6 H, CH_2N / CH_2OH / CH_2OBn), 4.50 (br. s, 2 H, CH_2Ph), 7.33–7.35 (m, 5 H, *arom. H*).	18.6 (s, CqCH$_3$), 28.1, 79.9, 157.7 (3s, *Boc*), 37.5 (s, N*Me*), 42.3 (s, *Cq*), 51.7 (s, CH_2N), 64.9 (s, CH_2OH), 73.1, 74.2 (2s, CH_2OBn / CH_2Ph), 127.2–138.2 (*arom. C*).
2k	0.77 (s, 3 H, CqCH_3), 1.45 (s, 9 H, *Boc*), 2.91 (s, 3 H, N*Me*), 3.35–3.52 (m, 6 H, CH_2N / CH_2OH).	18.0 (s, CqCH$_3$), 28.0, 80.3, 157.8 (3s, *Boc*), 38.0 (s, N*Me*), 41.7 (s, *Cq*), 52.2 (s, CH_2N), 68.1 (s, CH_2OH).
2l	0.82 (s, 3 H, CqCH_3), 1.40 (s, 9 H, *Boc*), 3.32–3.61 (m, 6 H, CH_2N / CH_2OH), 4.49 (s, 2 H, CH_2Ph), 7.20–7.39 (m, 5 H, *arom. H*).	18.8 (s, CqCH$_3$), 28.6, 81.5, 157.8 (3s, *Boc*), 42.4 (s, *Cq*), 50.5, 53.9 (2s, CH_2N / CH_2Ph), 69.1 (s, CH_2OH), 127.2–138.6 (*arom. C*).

As an alternative to the above autoclave procedure (Scheme 3), we envisaged the reaction of oxetanes with Li piperidide. With the parent oxetane $(CH_2)_3O$, this reaction has been found to produce 3-piperidinopropan-1-ol[13]. This type of reaction is limited to some specific amide reagents[13]. The substituted oxetanes **1a** and **1c** were found to incorporate the piperidyl residue with concomitant opening of the oxetane ring to produce **2h** and **2i** (Scheme 4). The products were obtained after distillation as analytically pure, light-yellow oils. Their ^{1}H- and ^{13}C-NMR spectral data were fully consistent with the proposed structures (Table 2).

Scheme 4. Cleavage of oxetanes by Li–piperidide

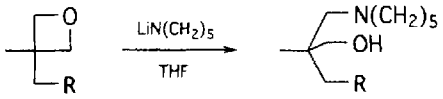

1 **2**

	R	yield (%)[a]
2h	OH	75
2i	OMe	41

[a] Analytically pure product after distillation through a 20-cm Vigreux column.

While the yields from this type of reaction (Scheme 4) are reasonable, the scope of the reaction is rather limited: Li–piperidide may not only act as a nucleophile as desired, but may also act as a strong base or as an electron-transfer reagent. Both these latter properties of the amide lead to complications when more demanding substituents R are present in **1**. When **1f**, bearing R = SCH_2Ph as the substituent, was treated with $LiN(CH_2)_5$, the tetrahydrothiophene derivative **A** (Scheme 5) was formed in over 90% yield.

Scheme 5. Reactions induced by Li–piperidide acting as a base (**A**) or as an electron-transfer reagent (**B**)

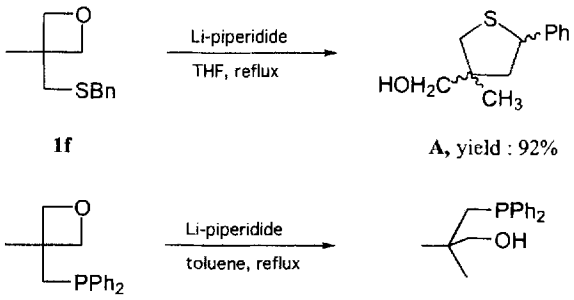

1f **A**, yield : 92%

1g **B**, yield : 19%

The identity of **A** was inferred from appropriate elemental analysis data, mass spectrometry and NMR spectrometry (see Experimental Section). The NMR spectra of **A** show that the two diastereomeric racemates are obtained in a 1:1 ratio with no diastereomeric discrimination whatsoever. The formation of **A** from **1f** is explained by deprotonation of the SCH_2Ph group as the initiating step[14]. The carbanion formed in this way will open the oxetane ring via an intramolecular nucleophilic attack. Interestingly, the product **A** is a constitutional isomer of the starting compound **1f**.

When **1g** (R = PPh_2) is used as the starting compound, reaction with Li–piperidide in THF or toluene leads to a mixture of products, with **B** being the only product isolated in yields of the order of 20% (Scheme 5). The reaction **1g** → **B** corresponds to a reduction process, which is obviously brought about by Li–piperidide acting as an electron-transfer reagent. Opening of the oxetane ring in **1** by Li–piperidide is thus of rather limited scope for the synthesis of tripod ligands.

It was thus decided to concentrate on the approach based on introduction of the nitrogen nucleophile in an autoclave reaction, as described above. Compounds **2a** and **2h**, bearing two OH functions and a tertiary amine group, could be *O*-mesylated. Reaction of the corresponding dimesylates with 2 equivalents of $LiPPh_2$ afforded **3a** and **3b** in good yields. Compounds **2b** and **2c**, bearing two OH groups and a secondary amine function, call for protection of this function prior to mesylation (Scheme 6).

Scheme 6. Transformations of the diols **2** into tripod ligands **3**

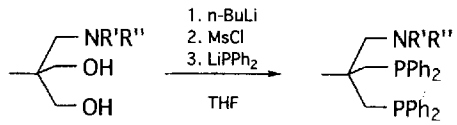

2 **3**

	NR'R''	yield (%)
3a	NMe_2	67
3b	$N(CH_2)_5$	70
3h	NMeBoc	34
3i	NBnBoc	34

Under standard conditions[15], the precursors **2b**, **c**, **e** were transformed into the Boc-protected products **2j**, **k**, **l** in high yield (Scheme 7).

Scheme 7. Boc protection of neopentane-derived secondary amines

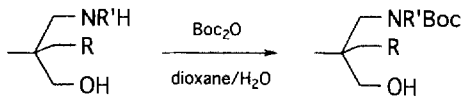

2b, c, e **2j, k, l**

	R	R'	yield (%)
2j	OBn	Me	82
2k	OH	Bn	88
2l	OH	Me	90

The ^{1}H- and ^{13}C-NMR spectra showed all the required groups of signals in each case. The CH_2 groups of the neopentane scaffolding give rise to overlapping multiplets integrating as six protons as expected (Table 3). The corresponding ^{13}C signals are clearly resolved, although unequivocal assignment to a specific CH_2X group is not always possible using 1D-spectroscopy (200 MHz).

Table 3. ^{1}H-, ^{13}C-, and ^{31}P-NMR spectra (solvent $CDCl_3$) of **3a–3i**

	^{1}H NMR [δ values]	^{13}C NMR [δ values]	^{31}P NMR [δ]
3a	0.92 (s, 3 H, CqCH_3), 2.29 (s, 6 H, NMe_2), 2.40 (m, 4 H, CH_2P), 2.47 (s, 2 H, CH_2N), 7.29–7.47 (m, 20 H, *arom. H*).	26.1 (t, $^3J_{CP}$ = 9.2 Hz, CqCH_3), 39.7 (br. s, *Cq*), 39.8 (m, CH_2P), 48.6 (s, NMe_2), 69.3 (t, $^3J_{CP}$ = 9.2 Hz, CH_2N), 128.0–140.1 (*arom. C*).	−27.2 (s)
3b	0.84 (s, 3 H, CqCH_3), 1.38, 1.46, 2.48 (3m, 2 H, 4 H, 4 H, *piperidine*-CH_2), 2.36 (m, 4 H, CH_2P), 2.42 (s, 2 H, CH_2N), 7.27–7.45 (m, 20 H, *arom. H*).	26.8 (br. s, CqCH_3), 24.7, 27.2, 57.9 (3s, *piperidine-C*), 40.2 (m, CH_2P), 40.9 (s, *Cq*), 68.6 (m, CH_2N), 128.6–140.8 (*arom. C*).	−26.9 (s)
3c	1.01 (s, 3 H, CqCH_3), 2.02 (s, 3 H, N*Me*), 2.38 (m, 4 H, CH_2P), 2.48 (s, 2 H, CH_2N), 7.27–7.48 (m, 20 H, *arom. H*).	26.8 (br. s, CqCH_3), 35.5 (s, N*Me*), 38.5 (s, *Cq*), 40.0 (m, CH_2P), 61.2 (s, CH_2N), 128.8–139.6 (*arom. C*).	−27.4 (s)
3d	1.02 (s, 3 H, CqCH_3), 2.41 (m, 4 H, CH_2P), 2.60 (s, 2 H, CH_2N), 3.42 (s, 2 H, CH_2Ph), 7.13–7.89 (m, 20 H, *arom. H*).	26.9 (br. s, CqCH_3), 39.3 (m, *Cq*), 40.7 (m, CH_2P), 54.8 (s, CH_2Ph), 59.3 (m, CH_2N), 127.0–141.2 (*arom. C*).	−26.9 (s)
3e	0.99 (s, 3 H, CqCH_3), 1.25 [d, 6 H, $^3J_{HH}$ = 6.0 Hz, CH(CH_3)], 2.33 (s, 6 H, NMe_2), 2.36 (m, 2 H, CH_2P), 2.36 (m, 2 H, CH_2N), 2.75 (s, 2 H, CH_2S), 2.76 [sept, 1 H, $^3J_{HH}$ = 6.0 Hz, CH(CH$_3$)], 7.31–7.56 (m, 10 H, *arom. H*).	23.4 (s, CqCH_3), 24.5, 24.6 [2s, CH(CH_3)], 36.3 [s, CH(CH$_3$)], 37.9 (d, $^3J_{CP}$ = 14.8 Hz, CH_2S), 40.1 (d, $^2J_{CP}$ = 13.0 Hz, *Cq*), 40.8 (d, $^1J_{CP}$ = 11.1 Hz, CH_2P), 48.6 (s, NMe_2), 67.8 (d, $^3J_{CP}$ = 9.2 Hz, CH_2N), 128.0–140.1 (*arom. C*).	−27.5 (s)
3f	1.00 (s, 3 H, CqCH_3), 2.32 (s, 6 H, NMe_2), 2.36 (m, 2 H, CH_2P), 2.40 (m, 2 H, CH_2N), 2.72 (s, 2 H, CH_2S), 3.70 (s, 2 H, CH_2Ph), 7.30–7.57 (m, 15 H, *arom. H*).	25.1 (d, $^3J_{CP}$ = 9.2 Hz, CqCH_3), 38.2 (s, CH_2Ph), 38.6 (br. s, CH_2S), 41.0 (d, $^2J_{CP}$ = 14.7 Hz, *Cq*), 42.9 (d, $^3J_{CP}$ = 11.0 Hz, CH_2P), 49.1 (s, NMe_2), 68.3 (d, $^3J_{CP}$ = 7.3 Hz, CH_2N), 127.3–140.6 (*arom. C*).	−26.9 (s)
3g	0.93 (s, 3 H, CqCH_3), 1.19 (m, 1 H, S*H*), 2.33 (s, 6 H, NMe_2), 2.35 (m, 2 H, CH_2P), 2.40 (m, 2 H, CH_2N), 2.74 (s, 2 H, CH_2S), 7.25–7.57 (m, 10 H, *arom. H*).	24.6 (d, $^3J_{CP}$ = 9.2 Hz, CqCH_3), 34.4 (d, $^3J_{CP}$ = 11.0 Hz, CH_2S), 37.4 (d, $^1J_{CP}$ = 16.5 Hz, CH_2P), 40.7 (m, *Cq*), 49.2 (s, NMe_2), 67.7 (d, $^3J_{CP}$ = 7.4 Hz, CH_2N), 128.8–140.5 (*arom. C*).	−27.4 (s)
3h	0.92 (s, 3 H, CqCH_3), 1.41 (s, 9 H, *Boc*), 2.27, 2.47, 3.34 (3m, 6 H, CH_2P / CH_2N), 2.89 (s, 3 H, N*Me*), 7.27–7.49 (m, 20 H, *arom. H*).	21.8 (br. s, CqCH_3), 28.7, 80.3, 158.0 (3s, *Boc*), 36.3 (m, CH_2P), 38.9 (s, N*Me*), 41.9 (m, *Cq*), 55.8, 68.0 (2s, CH_2N), 128.9–140.0 (*arom. C*).	−28.3 (s)
3i	1.02 (s, 3 H, CqCH_3), 1.41 (s, 9 H, *Boc*), 2.39 (m, 4 H, CH_2P), 3.44 (s, 2 H, CH_2N), 4.51 (s, 2 H, CH_2Ph), 7.13–7.49 (m, 20 H, *arom. H*).	26.7 (br. s, CqCH_3), 28.7, 80.4, 157.4 (3s, *Boc*), 40.8 (m, CH_2P), 41.9 (m, *Cq*), 54.0 (br. s, CH_2Ph), 58.2 (s, CH_2N), 127.3–140.2 (*arom. C*).	−28.0 (s)

The Boc-protected species **3h** and **3i** were obtained from **2k** and **2l** after analogous mesylation and substitution steps. The tripodal systems **3** – after purification by chromatography – are colourless, highly viscous oils. **3a** tends to crystallize upon prolonged storage at room temperature. The ^{1}H- and ^{13}C-NMR spectra of **3a, b, h, i** are diagnostic of the proposed structures (Table 3). Even though the methylene proton signals of the neopentane scaffolding give rise to separated signals (Table 3), the overlap between the signals and the low resolution (200 MHz) do not allow an assignment of individual coupling constants. The Boc-protected compounds **3h/3i**, effectively bearing amide nitrogen functions, show a clear differentiation of the CH_2N and CH_2P signals (Table 3). The PCH_2 protons give rise to complicated multiplet patterns (Table 3). The other groups present in **3a, b, h, i** all exhibit their characteristic patterns. The ^{13}C-NMR data with the appropriate J_{CP} coupling constants[5h] allows a clear distinction to be made between phosphorus-bound and nitrogen-bound groups (Table 3). The equivalence of the two PPh_2 substituents is evidenced by the appearance of just one sharp signal in the ^{31}P-NMR spectra in each case (Table 3).

Deprotection of **3h/3i** under standard conditions[15] led to **3c/3d** as tripod ligands having two equivalent phosphorus donors and a secondary amine as the third donor function (Scheme 8).

The identity of these products was verified by their ^{1}H-, ^{13}C-, and ^{31}P-NMR data (Table 3). A characteristic shift of the nitrogen-bound CH_2 group from δ ca. 3.4 in the Boc-protected precursor to δ ca. 2.4 in the deprotected products was observed.

Scheme 8. Deprotection of **3h, i**

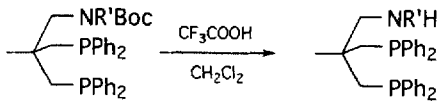

3h, i **3c, d**

	R′	yield [%]
3c	Me	99
3d	Bn	97

Compounds **2f** and **2g**, containing a tertiary amine group, a sulfur donor function and an OH group are amenable to a straightforward replacement of the OH group by a PPh_2 group by a sequence of deprotonation, mesylation and PPh_2 substitution steps (Scheme 9). After chromatography, the products **3e** and **3f** were obtained in high yields as colourless, viscous oils.

The benzyl thioether function in **3f** may be viewed as a benzyl-protected thiolate function, since methods for the reductive cleavage of an SBn bond in the presence of aryl bonds are known[9]. The procedure designed for other neopentane-based tripod ligands[9] works equally well for **3f**, which upon treatment with Li/NH_3/THF followed by hydrolytic work-up gives the functionalized thiol **3g** in almost

Scheme 9. Synthesis of chiral tripod ligands containing a P/N/S donor set

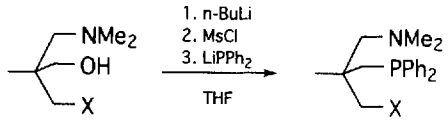

2 3

	X	yield (%)
3e	S*i*Pr	84
3f	SBn	77

80% yield (Scheme 10). As with the other compounds of type **3**, the ^{1}H-, ^{13}C-, and ^{31}P-NMR spectra convincingly prove the constitutions of **3e**, **3f**, **3g** (Table 3). The SH signal expected for **3g** is observed as a multiplet at δ = 1.19 (Table 3).

Scheme 10. Reductive cleavage of an SBn function in the presence of PPh_2 functionalities

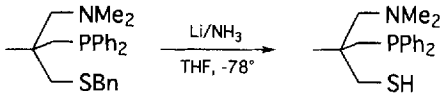

3f **3g**, yield : 78%

Coordination Chemistry

All compounds of type **3** are potential tripod ligands. The presence of hard and soft donor functions within the same tripod ligand might on the other hand preclude a trihapto binding mode, since hard and soft ligand functions do not generally fit well to a common ML_n fragment. In fact, it has been observed that η^3-bonding of neopentane-based tripod ligands containing two PPh_2 donor functions and one OR or SR group as the third donor function is not realized when these ligands are treated with $LM(CO)_3$ (M = Cr/Mo/W, L = ligands prone to substitution such as $(CO)_3$, $(CH_3CN)_3$, cycloheptatriene)[5a][5b]. Instead, $M(CO)_4$ derivatives with exclusively η^2-coordinated ligands are formed, with only the phosphorus functions involved in coordination[5a][5b]. This observation was generalized in the following statement: "clearly, a hard donor function cannot be forced to coordinate to a group VI metal center, not even through a tripodal linkage"[5b]. It is shown here that while η^2-coordination of $Mo(CO)_4$ by the tripod ligands with preferred coordination of the soft donor functions is a possible result (compounds **4**, Scheme 11), η^3-coordination of $Mo(CO)_3$ by the same ligands, with simultaneous coordination of hard and soft donor functions, is also quite feasible (compounds **5**, Scheme 12).

When compounds **3a**–**f** were treated with $(CH_3CN)_3Mo(CO)_3$[16] at 20°C, mixtures of complexes containing $Mo(CO)_4$ and $Mo(CO)_3$ species were obtained. Selective preparation of the $Mo(CO)_4$-containing species was achieved by refluxing **3a**–**f** with $Mo(CO)_6$ in toluene (Scheme 11).

Scheme 11. Dihapto binding mode of ligands **3** with the amine function acting as the dangling arm

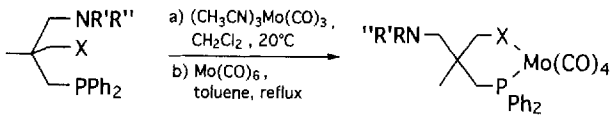

3 4

	NR'R''	X
4a	NMe_2	PPh_2
4b	$N(CH_2)_5$	PPh_2
4c	NMeH	PPh_2
4d	NBnH	PPh_2
4e	NMe_2	S*i*Pr
4f	NMe_2	SBn

The species **4** were isolated after evaporation of the solvent and elution of $Mo(CO)_6$ with petroleum ether (40–60), as light-brown powders in yields in excess of 60%. They were purified by recrystallization from CH_2Cl_2/petroleum ether (40–60), yielding yellow crystalline materials of analytical purity in the case of **4a**, **b**, **e**, **f**, while **4c**, **d** were precipitated as microcrystalline solids. Mass spectra (consecutive loss of up to four CO fragments) and ν_{CO} IR bands were in accord with the constitution as shown for **4** (Table 4). The ^{31}P-NMR spectra of **4a**–**f** reveal the presence of just one type of phosphorus nucleus in each case (Table 5).

Table 4. MS and IR spectra of **4** and **5**

	[M$^+$]	[M$^+$ − CO]	[M$^+$ − 2 CO]	[M$^+$ − 3 CO]	[M$^+$ − 4 CO]	IR$_{\nu CO}$ (CH_2Cl_2) [cm^{-1}]
4a	692 (3%)	664 (51%)	636 (100%)	608 (59%)	578 (85%)	2019 (s), 1903 (vs, br)
4b	721 (7%)	693 (30%)	665 (24%)	637 (51%)	609 (100%)	2018 (s), 1904 (vs, br)
4c	677 (15%)	650 (28%)	622 (50%)	594 (31%)	566 (100%)	2020 (s), 1901 (vs, br)
4d	755 (5%)	727 (25%)	699 (36%)	670 (65%)	642 (100%)	2019 (s), 1900 (vs, br)
4e	582 (23%)	554 (39%)	526 (82%)	498 (33%)	468 (97%)	2017 (s), 1898 (vs, br)
4f	631 (26%)	603 (25%)	574 (22%)	546 (23%)	519 (100%)	2019 (s), 1890 (vs, br)
5a	651 (18%)	623 (23%)	595 (17%)	567 (68%)		1924 (vs), 1805 (s, br)
5b	725 (14%)	697 (5%)	669 (6%)	641 (19%)		1924 (vs), 1813 (s, br)
5c	555 (59%)	527 (78%)	499 (25%)	471 (65%)		1922 (vs), 1803 (s, br)

For compounds **4a**–**4d**, this means that both the phosphorus centers present in the compounds **3a**–**3d** are coordinated and, therefore, that the amine function is not coordinated. For compounds **3e** and **3f**, with only one phosphorus donor, even a combination of ^{1}H- and ^{13}C-NMR spectral data does not unambiguously indicate whether the sulfur function or the nitrogen function is coordinated. Almost all of the CH_2 groups of the neopentane framework show multiplets for diastereotopically differentiated protons (Table 5). While such a differentiation is not evident for the

Table 5. ^{1}H-, ^{13}C- and ^{31}P-NMR spectra of **4a–4f** [a]

	^{1}H NMR [δ values]	^{13}C NMR [δ values]	^{31}P NMR [δ]
4a	0.65 (s, 3 H, CqCH_3), 2.15 (br. s, 2 H, CH_2N), 2.34 (s, 6 H, NMe_2), 2.55 (m, 4 H, CH_2P), 7.27–7.81 (m, 20 H, *arom. H*).	25.7 (br. s, CqCH_3), 39.8 (m, CH_2P), 40.3 (s, *Cq*), 48.8 (s, NMe_2), 75.7 (s, CH_2N), 128.0–140.7 (*arom. C*), 209.3, 215.3 (2m, *CO*).	+17.9 (s)
4b	0.61 (s, 3 H, CqCH_3), 1.46, 1.59, 2.51 (3m, 2 H, 4 H, 4 H, *piperidine-*CH_2), 2.16 (br. s, 2 H, CH_2N), 2.50 (m, 4 H, CH_2P), 7.27–7.87 (m, 20 H, *arom. H*).	24.8 (t, $^3J_{CP}$ = 5.5 Hz, CqCH_3), 23.7, 26.5, 57.4 (3s, *piperidine-C*), 36.7 (m, CH_2P), 40.6 (br. s, *Cq*), 74.5 (t, $^3J_{CP}$ = 9.2 Hz, CH_2N), 128.0–133.0 (*arom. C*).	+16.4 (s)
4c	0.88 (s, 3 H, CqCH_3), 2.17 (br. s, 2 H, CH_2N), 2.40 (s, 3 H, N*Me*), 2.70 (br. s, 4 H, CH_2P), 7.20–7.66 (m, 20 H, *arom. H*).	29.2 (br. s, CqCH_3), 37.8 (s, N*Me*), 38.2 (s, *Cq*), 38.3 (m, CH_2P), 54.0 (s, CH_2N), 125.8–139.7 (*arom. C*), 210.9, 215.6 (2m, *CO*).	+18.6 (s)
4d	0.80 (s, 3 H, CqCH_3), 2.37 (br. s, 2 H, CH_2N), 2.53, 2.65 (2dd, 4 H, $^2J_{HH}$ = 14.7 Hz, $^2J_{HP}$ = 8.9/7.8/4.8/5.5 Hz, CH_2P), 3.62 (s, 2 H, CH_2Ph), 7.29–7.74 (m, 25 H, *arom. H*).	28.0 (t, $^3J_{CP}$ = 7.0 Hz, CqCH_3), 37.8 (t, $^1J_{CP}$ = 11.2 Hz, CH_2P), 39.3 (br. s, *Cq*), 54.9 (s, CH_2Ph), 63.8 (t, $^3J_{CP}$ = 7.4 Hz, CH_2N), 127.5–140.9 (*arom. C*), 210.4, 211.5, 216.0 (3m, *CO*).	+17.8 (s)
4e	0.73 (s, 3 H, CqCH_3), 1.42 [d, 6 H, $^3J_{HH}$ = 6.5 Hz, CH(CH_3)], 2.06, 2.25 (2d, 2 H, $^2J_{HH}$ = 14.0 Hz, CH_2N), 2.28 (s, 6 H, NMe_2), 2.33, 2.56 (2d, 2 H, $^2J_{HH}$ = 14.0 Hz, CH_2P), 2.69, 2.88 (2d, 2 H, $^2J_{HH}$ = 11.3 Hz, CH_2S), 3.02 [sept, 1 H, $^3J_{HH}$ = 6.5 Hz, CH(CH$_3$)], 7.35–7.77 (m, 10 H, *arom. H*).	21.5 (s, CqCH_3), 25.9, 26.0 [2s, CH(CH_3)], 38.7 (d, $^1J_{CP}$ = 14.7 Hz, CH_2P), 40.8 (br. s, *Cq*), 43.6 [d, $^3J_{CP}$ = 7.4 Hz, CH(CH$_3$)], 46.6 (d, $^3J_{CP}$ = 5.5 Hz, CH_2S), 49.3 (s, NMe_2), 72.0 (d, $^3J_{CP}$ = 9.2 Hz, CH_2N), 128.6–140.1 (*arom. C*), 209.1, 210.1 (2d, $^2J_{CP}$ = 8.3 Hz, *CO trans* CO), 216.9 (d, $^2J_{CP}$ = 25.7 Hz, *CO trans* P), 217.1 (d, $^2J_{CP}$ = 9.2 Hz, *CO trans* S).	+15.3 (s)
4f	0.69 (s, 3 H, CqCH_3), 2.03, 2.15 (2d, 2 H, $^2J_{HH}$ = 14.0 Hz, CH_2N), 2.13 (s, 6 H, NMe_2), 2.29, 2.67 (2d, 2 H, $^2J_{HH}$ = 14.0 Hz, CH_2P), 2.62, 2.79 (2d, 2 H, $^2J_{HH}$ = 11.3 Hz, CH_2S), 4.05 (m, 2 H, CH_2Ph), 7.39–7.87 (m, 15 H, *arom. H*).	25.3 (d, $^3J_{CP}$ = 3.7 Hz, CqCH_3), 38.0 (d, $^1J_{CP}$ = 14.7 Hz, CH_2P), 40.7 (br. s, *Cq*), 46.5 (d, $^3J_{CP}$ = 5.5 Hz, CH_2S), 49.0 (s, NMe_2), 50.0 (d, $^3J_{CP}$ = 5.5 Hz, CH_2Ph), 72.2 (d, $^3J_{CP}$ = 11.0 Hz, CH_2N), 128.6–140.4 (*arom. C*), 209.0, 210.3 (2d, $^2J_{CP}$ = 8.3 Hz, *CO trans* CO), 216.1 (d, $^2J_{CP}$ = 27.6 Hz, *CO trans* P), 217.4 (d, $^2J_{CP}$ = 9.1 Hz, *CO trans* S).	+16.4 (s)

[a] Solvent CD_2Cl_2; the CD_2Cl_2 was condensed into the NMR tubes prior to flame-sealing.

ligand precursors and is completely absent for the CH_2SR groups (Table 3), the diastereotopic differentiation is clearly increased when part of the ligand is fixed by forming a six-membered chelate ring. The assignments given in Table 5 for the CH_2N and CH_2S fragments, respectively, rely solely on one-dimensional spectroscopic data and are largely based on the argument that the CH_2 group proximal to a coordinated donor function should show a lowfield NMR shift. Assuming that the CH_2S function is coordinated, the data are consistent with this expectation. The NCH_2 group thus assigned shows an unexpected highfield shift (Tables 3/5) of up to $\Delta\delta = 0.3$ in the dangling arm. While the assignment is not completely unambiguous, the X-ray analysis of the compounds (see below) supports this assignment in as much as the sulfur function is found to be coordinated whilst the amine function is not. The ^{13}C-NMR spectra of **4e** and **4f** show the presence of four chemically distinct carbonyl groups. The two non-equivalent equatorial CO groups *trans* to P and *trans* to S are characterized as such by their respective shifts and P–C coupling constants (Table 5). The two remaining signals, which are only separated by 1 ppm in each compound (Table 5), are assigned to the two axial carbonyl groups, which are differentiated by the chirality of the ligand. The discrimination between the two enantiotopic positions of these carbonyl groups can be understood in terms of a twist conformation of the chelate cycle, as observed in the X-ray structure determinations of these compounds (see below).

The tetracarbonylmolybdenum derivatives **4** could also be obtained from **3a–f** using $Mo(CO)_6$ as the starting compound (Scheme 11, see Experimental Section). No tricarbonylmolybdenum derivatives were formed under these conditions. In contrast, reaction of the same ligands **3a–f** with $(CH_3CN)_3Mo(CO)_3$ led to mixtures, the presence of tricarbonyl derivatives in which was indicated by the IR spectra (see above). The isolation of the corresponding tricarbonylmolybdenum derivatives containing the ligands in an η^3-binding mode was achieved by performing the reactions of **3c–3e** with $(CH_3CN)_3Mo(CO)_3$ in CH_2Cl_2 at −70°C. Such reactions are initially heterogeneous, with $(CH_3CN)_3Mo(CO)_3$ being almost insoluble in CH_2Cl_2 at −70°C. In the presence of the ligands **3**, the precipitate slowly dissolves over a period of hours and yellow solutions of **5** are formed. On removal of the solvent at −70°C, yellow powders remain, which upon crystallization from CH_2Cl_2/petroleum ether (40–60) give **5a–5c** in fair yields, in the form of analytically pure yellow crystals (Scheme 12).

Scheme 12. Trihapto coordination of tripod ligands containing a combination of hard and soft donor functions

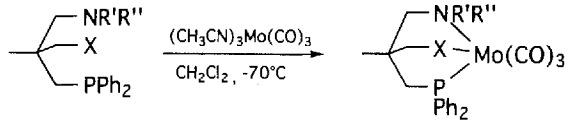

3 **5**

	NR′R″	X
5a	NMeH	PPh_2
5b	NBnH	PPh_2
5c	NMe_2	S*i*Pr

Mass spectra and ν_{CO} IR bands are in accord with the proposed structure for **5** (Table 4). The ^{31}P-NMR spectra of **5a** and **5b** show the presence of two chemically distinct phosphane donors, with $^2J_{PP}$ coupling constants of around 20 Hz (Table 6). For **5c**, only one singlet is observed, as would be expected. The ^{1}H-NMR spectra of **5** allow the unambiguous assignment of the different groups, even though the patterns cannot be resolved completely at 200 MHz (Table 6).

Table 6. ^{1}H-, ^{13}C- and ^{31}P-NMR spectra of **5a**, **5b** and **5c**[a]

	^{1}H NMR [δ values]	^{13}C NMR [δ values]	^{31}P NMR [δ]
5a	1.29 (s, 3 H, CqCH_3), 2.11 (m, 1 H, CHH-P), 2.15 (m, 1 H, CHH-P), 2.24 (m, 1 H, CHH-N), 2.50 (m, 1 H, CHH-P), 2.51 (m, 1 H, CHHN), 2.64 (d, 3 H, $^3J_{HH}$ = 5.8 Hz, NMe), 2.88 (m, 1 H, CHH-P), 3.05 (m, 1 H, NH), 7.03–7.90 (m, 20 H, *arom. H*).	34.5 (t, $^3J_{CP}$ = 9.2 Hz, CqCH_3), 35.0, 35.2 (2d, $^1J_{CP}$ = 9.2 Hz, CH_2P), 37.5 (t, $^2J_{CP}$ = 7.3 Hz, *Cq*), 48.6 (d, $^3J_{CP}$ = 5.5 Hz, NMe), 62.1 (d, $^3J_{CP}$ = 7.4 Hz, CH_2N), 128.4–140.3 (*arom. C*).	+18.3, 20.4 (2d, $^2J_{PP}$ = 20.8 Hz)
5b	1.18 (s, 3 H, CqCH_3), 2.05, 2.16 (2m, 2 H, CH_2-P), 2.19, 2.38 (2m, 2 H, CH_2-P), 2.52, 2.78 (2m, 2 H, CH_2-N), 3.21 (m, 1 H, NH), 3.49 (dd, 1 H, $^2J_{HH}$ = 13.3 Hz, $^3J_{HH}$ = 10.4 Hz, CHH-Ph), 4.47 (dd, 1 H, $^2J_{HH}$ = 13.3 Hz, $^3J_{HH}$ = 2.7 Hz, CHH-Ph), 7.08–7.97 (m, 25 H, *arom. H*).	[b]	+18.8, 21.3 (2d, $^2J_{PP}$ = 19.9 Hz)
5c	1.18 (s, 3 H, CqCH_3), 1.44, 1.50 [2d, 6 H, $^3J_{HH}$ = 6.5 Hz, CH(CH_3)], 2.23–2.84 (m, 6 H, CH_2P / CH_2N / CH_2S) 2.46, 2.85 (2s, 6 H, NMe_2), 3.03 [sept, 1 H, $^3J_{HH}$ = 6.5 Hz, CH(CH$_3$)], 7.39–7.91 (m, 10 H, *arom. H*).	22.1, 22.3 [2s, CH(CH_3)], 33.8 (d, $^3J_{CP}$ = 9.2 Hz, CqCH_3), 35.5 (d, $^1J_{CP}$ = 9.2 Hz, CH_2P), 38.8 (d, $^2J_{CP}$ = 7.4 Hz, *Cq*), 39.7 (br. s, CH_2S), 43.3 [d, $^3J_{CP}$ = 5.5 Hz, CH(CH$_3$)], 60.1, 61.6 (2s, NMe_2), 73.1 (d, $^3J_{CP}$ = 5.5 Hz, CH_2N), 128.7–139.8 (*arom. C*).	+19.2 (s)

[a] Solvent CD_2Cl_2; the CD_2Cl_2 was condensed into the NMR tubes prior to flame-sealing. – [b] ^{13}C spectrum could not be obtained because of the low solubility of **5b** in CD_2Cl_2.

^{13}C- and ^{1}H{^{31}P}-NMR spectral data further corroborate the given assignments (Table 6, Scheme 12). The isolation of analytically pure, crystalline products has to date only been achieved with the ligands **3c–3e**, producing **5a–5c**. The ligands **3a**, **b**, **f** also react with $(CH_3CN)_3Mo(CO)_3$ in CH_2Cl_2 at −70°C to give yellow solutions. The ν_{CO} IR bands of these solutions [ν_{CO} (CH_2Cl_2) cm^{-1}]: **3a**, 1925 (vs), 1810 (s, br); **3b**, 1933 (vs), 1824 (s, br); **3f**, 1923 (vs), 1805 (s, br)] are characteristic of the presence of $Mo(CO)_3$ as the chromophoric group. When these solutions are concentrated to dryness, brown powders are formed, which only partly redissolve in dichloromethane. The solutions thus obtained no longer show the ν_{CO} IR two-band pattern characteristic of $Mo(CO)_3$ groups; ν_{CO} IR bands are still present, but their intensity is decreased and they are more numerous. While it is probable that compounds analogous to **5a–5c** are formed initially, an alternative explanation for the observed $Mo(CO)_3$ band pattern would be that the ligands are only η^2-coordinated and that the remaining position is occupied by acetonitrile acting as a ligand. A decision between these two alternatives is not possible at present.

Compounds **5a–5c** are sensitive to moisture and air, even in the solid state. Their stability in solution is limited and it is essential to prepare and handle their solutions at temperatures below 0°C. Their lability appears to be connected with the ease with which the nitrogen donor can be displaced. Thus, a CH_2Cl_2 solution of **5c** reacts spontaneously with CO (1 bar) to produce the tetracarbonyl species **4e** (Scheme 13). Irradiation of **4e** initiates photolytic decarbonylation, with the vacant coordination site thus produced allowing recoordination by the NMe_2 dangling arm (Scheme 13). The identity of **5c** and **4e**, as produced from these reactions, was substantiated by ^{31}P-NMR and ν_{CO} IR bands in each case (see Experimental Section).

Scheme 13. Interconversion of **5** and **4**

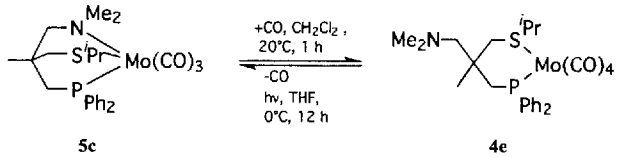

5c **4e**

X-ray Structures

In order to independently prove the connectivity schemes established for **4** on the basis of their NMR spectra, the structures of **4a**, **4b**, **4e**, and **4f** were determined by single-crystal X-ray analyses[17]. The connectivities observed for the molecules in the solid state (Figure 1) were found to be consistent with those inferred from NMR data for the same compounds in solution. The coordination environment of the metal is idealized octahedral. There are two crystallographically independent molecules in the crystal of **4f**, which are designated **4f/1** and **4f/2** (Table 7, Figure 1).

The scalar properties of all five different molecules of type **4** are closely similar where appropriate comparisons can be made (Table 7). Mo–P and Mo–S distances are also very similar. The Mo–C(CO) distances to the carbonyl groups *trans* to the heteroatoms (Mo–C41, Mo–C42) are consistently significantly shorter [194.9(5)–199.0(4) pm] than the distances found for the carbonyl groups *trans* to each other [201.8(6)–205.5(5) pm] (Table 7). The *trans*-effect of the phosphorus donor is not significantly different from the *trans*-effect of the sulfur donor function. While in **4e** the M–C(CO) distances *trans* to P and *trans* to S (Mo–C41, Mo–C42) are slightly different [197.2(5),

Figure 1. Conformations observed for **4a**, **4e** and **4f** in the solid state[a]

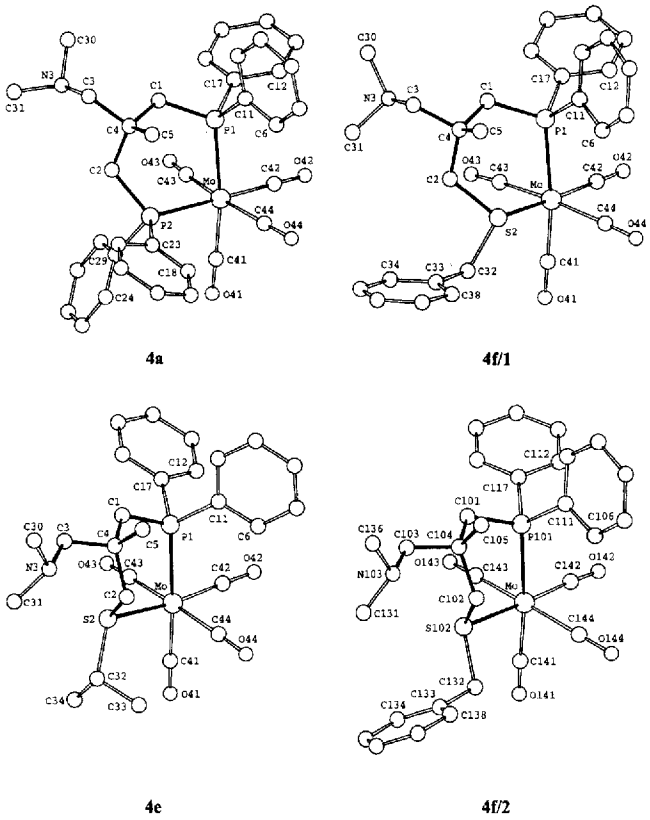

[a] **4f/1** and **4f/2** denote the two crystallographically independent molecules in the crystal of **4f**. The structure of **4b** corresponds in its overall arrangement to the structures shown for **4a** and **4f/1**. The chelate ring has chair conformation as in **4a** and in **4f/1** (see also Table 7).

194.9(5) pm], these distances are equal within the limits of error in **4f** (Table 7).

The bite angles of the different ligands vary between 82.4(1)° and 88.9(1)°. While the scalar properties are thus in almost quantitative agreement for all compounds **4**, the torsion angles characterizing the individual conformations are different (Table 7). Figure 1 shows the reason for this difference: While **4a** and **4f/1** have the chelate rings in a chair conformation (as does **4b**, not shown in Figure 1, data in Table 7), **4e** and **4f/2** show a twist-boat conformation of these rings. Hence, there are two classes of conformations. Columns **4a**, **4b**, and **4f/1** in Table 7 show the close agreement between the individual torsion angles characterizing this class of compounds, which have the chelate ring in a chair conformation. Analogously, columns **4e** and **4f/2** show the good agreement between their conformations, both having a twist-boat arrangement of the chelate ring (Figure 1, Table 7). The chair conformations (**4a**, **4b**, **4f/1**) are characterized by an approximate mirror symmetry, which relates the corresponding torsion angles in pairs such that angles related by this symmetry [Mo−P1−C1−C4, C4−C2−P2(S2)−Mo, etc.] are close in absolute value but opposite in sign (Table 7). For the twist-boat conformations (**4e**, **4f/2**), inherent C_1 symmetry does not call for any pairwise agreement (an idealized twist-boat conformation would impose C_2 symmetry). For the two different compounds **4e** and **4f**, both of which have their chelate rings in twist-boat conformations (**4e**, **4f/2**), the values of the torsion angles characterizing this conformation are quite similar (Table 7). All five molecules **4a**, **b** and **4e**, **4f/1**, **4f/2** have the PPh_2 donor group in common. Comparison of the arrangement of the phenyl rings of this group centered at P1 (Figure 1) suggests that the torsional arrangement of these groups is in fact very similar for all the compounds shown (Table 7). As measured relative to the Mo−P1 axis, the torsion angles around P1−C11 (P101−C111 in **4f/2**) fall in a narrow range from 6.3(3) to −22.1(4)°. The corresponding torsion angles characterizing the rotation of the second phenyl group at this phosphorus center are equally close to each other, lying between −68.3(4) and −83.3(3)° (Table 7). The comparison of **4a**, **4f/1** and **4e**, **4f/2** in Figure 1 suggests that the main difference in the appearance of the PPh_2 group at P1 (P101 in **4f/2**) is caused by a rotation of this group around the Mo−P axis. The torsion angles C44−Mo−P1−C1 (Table 7) confirm this idea. The different torsional arrangements required for the chair conformations (**4e** / **4f/2**) necessitate this torsion about the Mo−P bond. The torsional arrangement of the two PPh_2 groups present in each of **4a/4b** corresponds quite closely to the idealized mirror symmetry of these compounds (Table 7, Figure 1). In each case, the two different substituents at the carbon atom C4 (C104 in **4f/2**) are arranged such that the aminomethyl substituent points away from the center of the coordination polyhedron (Figure 1). This corresponds to an equatorial position in **4a**, **4b**, **4f/1** with respect to the chelate ring. The methyl group at C5 is pointing inward (Figure 1) and thus comes into close contact with one phenyl group at P1 (C11 in **4a**, **b**, **e**, **f/1**; C111 in **4f/2**) in each case. The distance between C5 (C105) and the center of this phenyl group measures between 368 pm (**4f/2**) and 413 pm (**4b**). Due to the close proximity of this phenyl ring and the methyl group, the rotational freedom of the phenyl group is obviously quite restricted. Consequently, very similar torsion angles Mo−P1−C11−C6 (Mo−P101−C111−C106 in **4f/2**) are found in all of the compounds (see above). The second phenyl group at this phosphorus has to adopt an orientation according to the given rotation of the first one. Thus, the torsion angles Mo−P1−C17−C12 (Mo−P101−C117−C112 in **4f/2**) are again quite close to each other for all the molecules **4** (Table 7). The rotational position occupied by the CH_2NR_2 substituent (rotation around C3−C4; C103−C104 in **4f/2**) corresponds to the idealized C_s-symmetry of the chair-type chelate arrangements in **4a**, **4b**, **4f/1** (Figure 1) with torsion angles C5−C4−C3−N3 close to 180° (Table 7). For the twist-boat conformations, these torsion angles respond to the skew of the twist conformation and the corresponding angles are close to 60°. Molecular models built for the compounds suggest that this difference in the orientation of the CH_2NR_2 groups is due to a minimization of the repulsive contacts between the NR_2 group and the other organic substituents.

Table 7. Selected bond distances [pm], bond angles [°] and torsion angles [°] for **4a**, **4b**, **4e**, and **4f**[a]

	4a	4b	4e	4f/1	4f/2
Mo1–P1	252.2(1)	254.1(2)	253.8(1)	252.8(1)	253.9(1)
Mo1–P2	254.7(2)	253.3(2)	–	–	–
Mo1–S2	–	–	256.7(1)	253.0(1)	256.4(1)
Mo1–C41	199.0(4)	198.2(6)	197.2(5)	198.0(4)	197.3(4)
Mo1–C42	198.8(4)	197.0(6)	194.9(5)	197.7(4)	197.1(4)
Mo1–C43	202.4(4)	205.2(7)	205.5(5)	203.4(4)	203.0(4)
Mo1–C44	204.7(4)	201.8(6)	203.4(6)	203.9(4)	204.1(4)
P1–Mo1–P2	88.9(1)	85.5(1)	–	–	–
P1–Mo1–S2	–	–	82.4(1)	83.0(1)	83.7(1)
Mo1–P1–C11–C6	6.3(3)	0.2(5)	0.7(5)	−14.7(4)	−22.1(4)
Mo1–P1–C17–C12	−83.3(3)	−70.6(5)	−68.3 (4)	−77.5(3)	−82.6(3)
Mo1–P2–C23–C18	−24.3(3)	−0.2(5)	–	–	–
Mo1–P2–C29–C24	115.4(3)	69.6(4)	–	–	–
C44–Mo1–P1–C1	−127.2(2)	−140.4(3)	−101.7(2)	−132.1(2)	−116.2(2)
Mo1–P1–C1–C4	58.2(3)	60.6(4)	61.4(4)	56.3(3)	70.4(3)
P1–C1–C4–C2	−76.4(3)	−65.7(6)	−38.5(5)	−62.4(4)	−37.8(4)
C1–C4–C2–P2(S2)	−71.2(3)	−66.1(5)	42.5(5)	−73.6(3)	44.1(4)
C4–C2–P2(S2)–Mo1	51.2(3)	61.5(4)	−89.6(3)	76.3(3)	−83.1(3)
C2–P2(S2)–Mo1–P1	−27.4(1)	−41.3 (2)	46.6(2)	−51.8(1)	35.4(1)
P2(S2)–Mo1–P1–C1	−29.4(1)	−41.0(2)	9.0(2)	−44.2(1)	−21.6(1)
C5–C4–C3–N3	−179.0(3)	−180.0(4)	−61.7(5)	178.3(3)	−57.7(4)

[a] **4f/1**, **4f/2** see legend to Figure 1. Compound **4b** is not shown in Figure 1. The numbering scheme is such that chemically equivalent atoms have the same numbers in molecules **4a**, **4b**, **4e**, **4f/1**; the numbering scheme adopted for **4f/2** relates chemically equivalent atoms by adding 100 to the numbers used in **4f/1** (not including molybdenum).

The substituents at the sulfur centers also occupy positions that reduce steric crowding within the molecules (Figure 1). The positions are equatorial in the chair conformations of **4a**, **b**, **f/1** and quasi-equatorial in the twist-boat conformations present in **4e**, **4f/2**. The chiral centers at C4 and S2 in **4f** have the same sense of chirality (*R*,*R*) in **4f/1**. In **4f/2**, the chirality at the sulfur center is (*S*), corresponding to an inversion at sulfur; the (*R*,*S*) isomer is thus formed. Of course, with the synthesis being non-enantioselective and the crystals not belonging to a chiral space group, both enantiomers are found in the crystal [(*R*,*R*)/(*S*,*S*) in **4f/1**, (*R*,*S*)/(*S*,*R*) in **4f/2**]. Accordingly, both enantiomers are found in the crystal of **4e**. The nomenclature for assigning absolute configurations[18] assigns (*S*) to the configuration at sulfur in **4f/2** and (*R*) to the sulfur configuration observed in **4e**, which might be somewhat misleading if not clarified here. The configuration in **4e** is thus designated as (*R*,*R*) while being almost equivalent to the (*R*,*S*) configuration of **4f/2** (Figure 1). Again both enantiomers are found in the crystal.

To probe the influence of two or three different donor functions in a neopentane-based tripod ligand, the structures of **5a**, **5b**, and **5c** were determined by X-ray crystallography (Figure 2, Table 8)[17]. It was of particular interest to see how the bicyclo[2.2.2]octane-type chelate cage would adapt to the presence of hard and soft donor functions and hence to donor atoms of quite different radii.

Figure 2 shows that the distortions caused by this inequivalence of donor functions are not particularly prominent at first glance, even though the Mo–P (Mo–S) distances differ from the Mo–N distances by around 15 pm (Table 8). The angles subtended at the metal by the donor atoms are smaller than 90° for the P–Mo–P as well as for the P–Mo–N, P–Mo–S, and S–Mo–N fragments (in **5b**, an angle of around 90° is found for the P–Mo–P arrangement; the standard deviation for this angle is quite good but there might be some systematic error introduced by the fact that the benzyl group in this compound shows disorder, even though this disorder is well-resolved in the structural analysis[17]). As already observed for compounds **4** (Table 7), neither the Mo–P and Mo–S distances nor the Mo–C(CO) distances relating to bonds *trans* to P or *trans* to S show any significant differences (Table 8).

The *trans*-effect of the nitrogen donors is indicated by the observation that the average Mo–C(CO) distances relating to carbonyl groups *trans* to nitrogen (Mo–C43) are shorter (193.5 pm) than the distances Mo–C41 and Mo–C42 (196.2 pm, see Table 8).

The three torsion angles (Table 8) describing the skew of the scaffolding, and thus characterizing the conformation of the chelate cage, are within the range of torsion angles previously observed for coordination compounds of $CH_3C(CH_2PPh_2)_3$[3a]. The rotational positions of the aryl groups at the PPh_2 donor centers observed in **5** merit some comment. The mutual arrangements of the two phenyl groups closest to each other at P1 and P2 (C11, C23) show a clear distinction. These rings are almost parallel in **5a** and almost vertical to each other in **5b**. The conventional torsion angles given in Table 8 do not appropriately describe what is apparent when looking at Figure 2. If a different convention, as given in the footnote to Table 8, is used to define these aryl torsions, the numbers are more easily interpreted[3a]. With this convention, the rotation about the P–C axis relative to an idealized C_3-axis of the $Mo(CO)_3$

Figure 2. Structures of **5a**, **5b**, and **5c** observed in the crystal

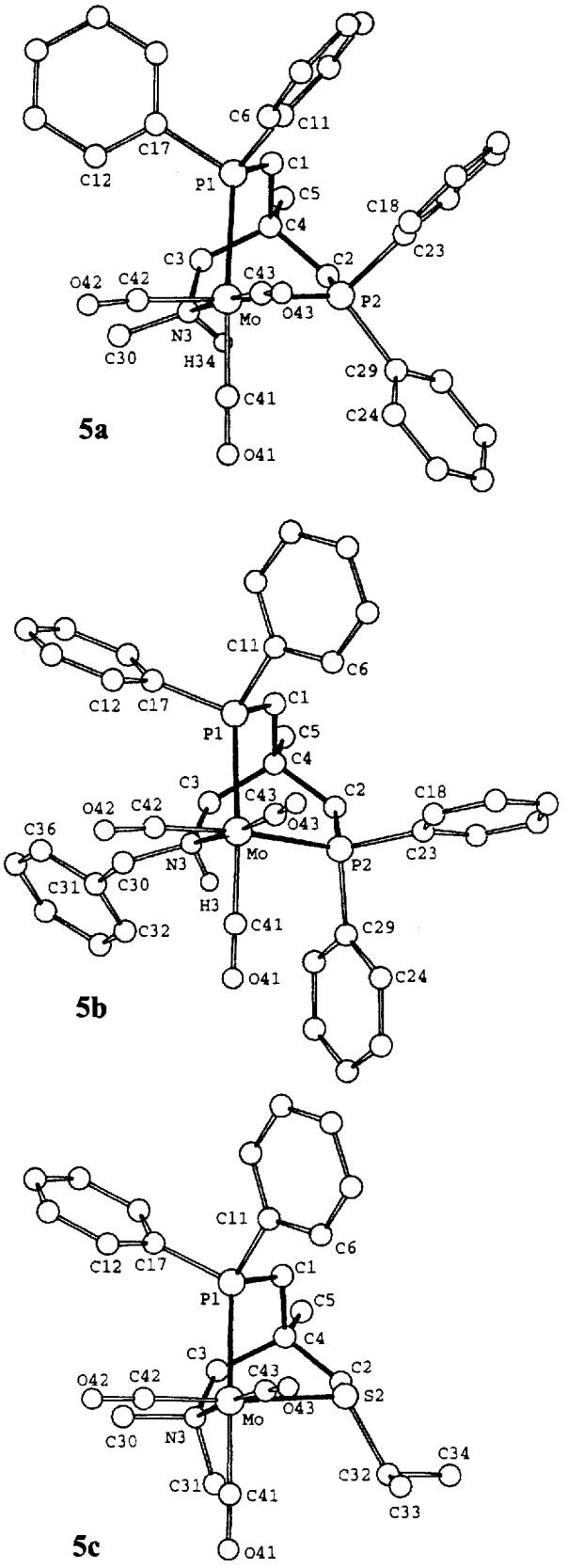

fragment (corresponding closely to the idealized C_3-axis of the chelate cage) is measured. Here, an angle of 0° corresponds to this axis being parallel to the ring plane, while a value of ±90° indicates that the corresponding phenyl group appears maximally extended in a projection along this axis. (The axis of projection used in Figure 2 is somewhat tilted with respect to the idealized axis in order to allow for a minimization of overlap in the two-dimensional projection.) The meaning of the torsion angles as defined above is still apparent from this kind of projection (Figure 2). The arrangement found in **5a** corresponds to a "parallel" approach of the two inner phenyl rings, while these two rings approach in a vertical mode in **5b** (see torsion angles at the bottom of Table 8). The torsion angles as defined show that the PPh_2 groups at P1 in **5b** and **5c** have very similar torsional arrangements. This is also intuitively clear from Figure 2.

Table 8. Selected bond distances [pm], bond angles [°] and torsion angles [°] for **5a**, **5b**, and **5c**[a]

	5a	**5b**	**5c**
Mo1–P1	255.7(2)	250.8(2)	253.0(1)
Mo1–P2(S2)	252.0(2)	253.4(2)	255.1(1)
Mo1–N3	236.3(6)	236.6(6)	239.1(3)
Mo1–C41	196.0(6)	196.4(8)	196.7(4)
Mo1–C42	199.5(6)	194.6(7)	194.0(4)
Mo1–C43	194.3(7)	192.9(8)	193.3(4)
P1–Mo1–P2(S2)	80.0(1)	90.1(1)	81.2(1)
P1–Mo1–N3	84.1(1)	80.2(2)	82.9(1)
P2(S2)–Mo1–N3	82.9(1)	79.2(2)	85.5(1)
Mo1–P1–C1–C4	20.6(5)	26.6(6)	29.0(3)
Mo–P2(S2)–C2–C4	36.3(5)	4.5(6)	36.4(3)
Mo–N3–C3–C4	38.5(7)	17.8(6)	32.4(4)
Mo1–P1–C11–C6	−51.1(6)	30.0(7)	28.6(4)
Mo1–P1–C17–C12	−15.6(6)	61.1(6)	57.2(3)
Mo1–P2–C23–C18	39.9(6)	8.1(7)	–
Mo1–P2–C29–C24	−32.0(6)	83.4(7)	–
H_z1–P1–C11–C6	−15.5	68.8	64.4
H_z1–P1–C17–C12	−55.9	14.6	11.9
H_z2–P2–C23–C18	−14.5	−34.2	–
H_z2–P2–C29–C24	−6.3	−46.8	–

[a] The torsion angles involving H_z at the bottom of the table are defined as follows: P–H_z designates a vector that is vertical to the plane formed by the three donor atoms and points towards the observer when in a projection onto this plane the vector Mo–C4 points away from the observer, that is C4 is below this plane (Figure 2)[3a]. The planes defined by the donor atoms of the tripod ligands in **5** are almost parallel to the planes defined by the carbon atoms of the $Mo(CO)_3$ fragment in each case.

In conclusion, tripod ligands $CH_3C(CH_2X)(CH_2Y)(CH_2Z)$ with one nitrogen donor group X and two equivalent phosphorus donor functions Y = Z = PR_2, or with one phosphorus and one sulfur donor function Y = PR_2, Z = SR, are readily accessible.

Such tripod ligands with two soft (P, S) and one hard (N) donor atoms tend to coordinate primarily in an η^2-binding mode to Mo^0, with the soft bases bound to the metal. The six-membered chelate rings thus formed adopt chair conformations when the donor functions are the same, but may have twist-boat conformations with dissimilar donor functions.

η^3-Coordination of tripod ligands with one nitrogen and two phosphorus donors, as well as those with one nitrogen,

one phosphorus, and one sulfur donor, is quite possible in tripod-$Mo(CO)_3$ coordination compounds. Under carbonylation conditions, carbonyl substitution of the nitrogen donor occurs selectively.

We are grateful to the *German Science Foundation (DFG), SFB 247*, the *VW Foundation (Stiftung Volkswagenwerk)* and the *Fonds der Chemischen Industrie* for financial support. The technical support of *Th. Jannack* (mass spectrometry) and the Microanalytical Laboratory of the Institute of Organic Chemistry is gratefully acknowledged.

Experimental Section

All manipulations involving phosphanes were carried out under an argon atmosphere by means of standard Schlenk techniques. – The aminolytic cleavage of oxetanes was carried out in a HR 100 stainless steel high-pressure laboratory reactor (Berghof/Maasen GmbH). – All solvents were dried by standard methods[19] and distilled under argon. The $CDCl_3$ and CD_2Cl_2 used for the NMR spectroscopic measurements were degassed by three successive "freeze-pump-thaw" cycles and dried over 4-Å molecular sieves. – NMR: Bruker Avance DPX 200 at 200.13 MHz (^1H), 50.323 MHz ($^{13}C\{^1H\}$), 81.015 MHz ($^{31}P\{^1H\}$); T = 298 K; chemical shifts (δ) in ppm with respect to the proton residues in $CDCl_3$ (^1H: δ = 7.27, ^{13}C: δ = 77.0) and CD_2Cl_2 (^1H: δ = 5.32, ^{13}C: δ = 53.5) as internal standards, and chemical shifts (δ) in ppm with respect to 85% H_3PO_4 (^{31}P: δ = 0) as external standard. – IR: Bruker FT-IR IFS-66; CaF_2 cells. – MS (EI): Finnigan MAT 8400. – Melting points: Gallenkamp MFB-595 010; melting points are uncorrected. – Elemental analysis: Microanalytical Laboratory of the Organisch-Chemisches Institut, Universität Heidelberg. The procedures used for determining the carbon content often gave falsely low values when Mo was present in the compound owing to the formation of incombustible Mo carbide. – The silica gel (Kieselgel z.A. 0.06–0.2 mm, J.T. Baker Chemicals B.V.) used for chromatography was degassed at 1 mbar for 24 h and saturated with argon. A solution of 2.5 M *n*BuLi in hexanes was used for deprotonations. $Mo(CO)_6$ was sublimed before use. $(CH_3CN)_3Mo(CO)_3$[16], **1a**[12a], **1b**[12b], **1c**[12c], **1d**[12d], and **1g**[5k] were prepared according to literature procedures. All other chemicals were obtained commercially and used without further purification.

X-ray Structure Determinations: The measurements for **4a**, **4b**, **4e**, **4f**, **5a**, **5b**, and **5c** were carried out on a Siemens P4 four-circle diffractometer (equipped with a low-temperature device) with graphite-monochromated Mo-K_α radiation. All calculations were performed using the SHELXT-PLUS[20] software package. Structures were solved by direct methods with the SHELXS-86 program[20a] and refined with the SHELX-93 program[20b]. Graphical handling of the structural data during solution and refinement was performed with XPMA[21]. An absorption correction (π-scan, $\Delta\psi = 10°$) was applied to all data. Atomic coordinates and anisotropic parameters of the non-hydrogen atoms were refined by full-matrix least-squares calculations. Data for the structure determinations are compiled in Table 9[17].

Ligand Syntheses

Oxetanes. – Preparation of **1e**, **1f**: 6.1 g (60 mmol) of **1b** was dissolved in 500 ml of THF. Meanwhile, 65 mmol of the thiol was deprotonated with 26 ml (65 mmol) of *n*BuLi solution in 200 ml of THF at 0°C. After 1 h, the solution of **1b** was added slowly to the Li–thiolate solution resulting in a voluminous white precipitate of lithium mesylate. The reaction mixture was stirred at room temperature for 12 h. THF was then removed by means of a rotary evaporator, the crude product was dissolved in 200 ml of Et_2O and washed with 100 ml of a saturated aqueous NaCl solution. The phases were separated and the aqueous phase was washed three times with Et_2O. The combined organic phases were dried with $MgSO_4$, the solvent was removed in vacuo, and the products were distilled under reduced pressure through a 15 cm Vigreux column, yielding oxetanes **1** as colourless liquids.

3-(Isopropylsulfanylmethyl)-3-methyloxetane (**1e**): Yield: 8.54 g (53.3 mmol, 89%), b.p. 94°C (23 Torr). – EI-MS; *m/z* (%): 160 (10) [M^+], 130 (11) [$M^+ - CH_2O$], 74 (100) [$SC_3H_7^+$], 54 (33) [$C_4H_6^+$]. – $C_8H_{16}OS$ (160.27): calcd. C 59.95, H 10.06, S 20.00; found C 60.00, H 10.21, S 19.95.

3-(Benzylsulfanylmethyl)-3-methyloxetane (**1f**)[9]: Yield: 10.65 g (51.1 mmol, 85%), b.p. 94°C (23 Torr). – EI-MS; *m/z* (%): 208 (10) [M^+], 125 (25) [SCH_2Ph^+], 91 (100) [$C_7H_7^+$]. – $C_{12}H_{16}OS$ (208.31): calcd. C 69.19, H 7.74; found C 68.67, H 7.66.

Amino Alcohols. – Preparation of **2a–g**: A mixture of 50 mmol of **1** and 125 mmol of amine (45% aqueous solution) was maintained at 150°C in an autoclave (for reaction times see Scheme 3). Aliquots were withdrawn at intervals and analyzed by ^1H NMR to monitor the progress of the reaction. Upon completion, the excess amine and water were removed in a rotary evaporator, and the residue was distilled at reduced pressure through a 20 cm Vigreux column (for % yields see Scheme 3).

2-(Dimethylaminomethyl)-2-methylpropane-1,3-diol (**2a**)[11]: Yield: 5.17 g (35.1 mmol), b.p. 90–93°C (0.7 Torr). – $C_7H_{17}NO_2$ (147.22): calcd. C 57.11, H 11.64; found C 56.85, H 11.41.

2-Methyl-2-(methylaminomethyl)propane-1,3-diol (**2b**): Yield: 5.73 g (43.1 mmol), b.p. 90–92°C (1 Torr). – EI-MS; *m/z* (%): 133 (100) [M^+], 103 (35) [$M^+ - NHMe$]. – $C_6H_{15}NO_2$ (133.11): calcd. C 54.11, H 11.35, N 10.52; found C 53.98, H 10.97, N 10.28.

2-(Benzylaminomethyl)-2-methylpropane-1,3-diol (**2c**): Yield: 5.42 g (25.9 mmol), b.p. 135–140°C (0.6 Torr). – EI-MS; *m/z* (%): 209 (3) [M^+], 120 (46) [$M^+ - Bn$], 91 (100) [$C_7H_7^+$]. – $C_{12}H_{19}NO_2 \cdot 1/5\ H_2O$ (209.29)*: calcd. C 67.70, H 9.19, N 6.58; found C 67.94, H 9.10, N 6.64; * water content: H_2O cannot be completely removed by distillation.

(±)-2-(Benzoxymethyl)-2-(dimethylaminomethyl)-2-methylpropan-1-ol (**2d**): Yield: 10.03 g (42.3 mmol), b.p. 140–145°C (1.1 Torr). – EI-MS; *m/z* (%): 237 (2) [M^+], 146 (11) [$M^+ - Bn$], 91 (12) [$C_7H_7^+$], 58 (100) [$C_4H_{10}^+$]. – $C_{14}H_{23}NO_2$ (237.34): calcd. C 70.85, H 9.77, N 5.90; found C 70.75, H 9.62, N 5.65.

(±)-2-(Benzoxymethyl)-2-methyl-2-(methylaminomethyl)-propan-1-ol (**2e**): Yield: 7.68 g (34.4 mmol), b.p. 150–153°C (1.3 Torr). – EI-MS; *m/z* (%): 223 (18) [M^+], 132 (59) [$M^+ - Bn$], 91 (100) [$C_7H_7^+$]. – $C_6H_{15}NO_2$ (223.32): calcd. C 69.92, H 9.48, N 6.27; found C 69.73, H 9.54, N 6.14.

(±)-2-(Dimethylaminomethyl)-2-(isopropylsulfanylmethyl)-2-methylpropan-1-ol (**2f**): Yield 7.79 g (38.0 mmol), b.p. 109°C (1.1 Torr). – EI-MS; *m/z* (%): 205 (15) [M^+], 162 (5) [$M^+ - NMe_2$], 130 (22) [$M^+ - SC_3H_7$], 100 (6) [$M^+ - CH_2OH - SC_3H_7$], 58 (100) [$C_4H_{10}^+$]. – $C_{10}H_{23}NOS$ (205.36): calcd. C 58.49, H 11.29, N 6.82; found C 58.71, H 11.25, N 6.33.

(±)-2-(Benzylsulfanylmethyl)-2-(dimethylaminomethyl)-2-methylpropan-1-ol (**2g**): Yield 6.81 g (26.9 mmol), b.p. 115°C (1 Torr). – $C_{14}H_{23}NOS$ (253.4): calcd. C 66.36, H 9.15, N 5.53, S 12.65; found: C 66.11, H 9.29, N 5.27, S 12.49.

Preparation of **2h**, **2i**: 3.36 g (40 mmol) of piperidine was deprotonated in 30 ml of THF with 16 ml (40 mmol) of *n*BuLi solution

Table 9. Crystal data for **4a**, **4b**, **4e**, **4f**, **5a**, **5b**, and **5c**

Compound	**4a**	**4b**	**4e**	**4f**	**5a**	**5b**	**5c**
Formula	$C_{35}H_{35}NO_4P_2Mo$	$C_{38}H_{39}NO_4P_2Mo$	$C_{26}H_{32}NO_4PSMo$	$C_{30}H_{32}NO_4PSMo$	$C_{33}H_{33}NO_3P_2Mo$	$C_{39}H_{37}NO_3P_2Mo$	$C_{25}H_{32}NO_3PSMo$
Molecular mass [g/mol]	691.55	721.54	581.52	629.56	649.52	725.62	553.51
Crystal size [mm]	0.3 × 0.3 × 0.3	0.3 × 0.4 × 0.3	0.3 × 0.2 × 0.2	0.3 × 0.2 × 0.4	0.3 × 0.3 × 0.3	0.2 × 0.2 × 0.15	0.4 × 0.25 × 0.25
crystal system	triclinic	triclinic	triclinic	triclinic	monoclinic	monoclinic	orthorhombic
space group (No.)[20c]	$P\bar{1}$ (No. 2)	$P1$ (No. 1)	$P\bar{1}$ (No. 2)	$P\bar{1}$ (No. 2)	$P2_1$ (No. 4)	$P2_1/n$ (No. 14)	$Pbca$ (No. 61)
a [pm]	942.6(4)	946.2(4)	912.0(2)	1066.4(5)	902.6(3)	984.7(1)	1652.3(1)
b [pm]	1078.9(2)	1079.0(4)	1213.2(2)	1690.8(6)	1527.3(5)	1676.2(6)	1538.9(5)
c [pm]	1750.0(7)	1082.3(4)	1308.6(3)	1886.6(6)	1155.6(3)	2075.7(3)	1996.2(2)
α [°]	106.14(3)	100.67(3)	84.89(1)	64.59(1)	90	90	90
β [°]	93.31(4)	111.33(5)	82.51(2)	87.35(1)	107.21(1)	98.44(1)	90
γ [°]	102.16(3)	110.98(3)	74.63(1)	88.46(2)	90	90	90
V [10^6 pm^3]	1658.3(1)	895.6(6)	1381.9(5)	3069.2(2)	1521.7(8)	3389.0(14)	5076(2)
Z	2	1	2	4	2	4	8
d_x [g cm^{-3}]	1.385	1.356	1.397	1.407	1.417	1.422	1.449
T [K]	200	200	200	200	200	200	200
no. rflns. for cell param. refinm.	25	25	25	25	25	33	39
scan range	4.5° ≤ 2Θ ≤ 46.0°	4.3° ≤ 2Θ ≤ 50.0°	4.6° ≤ 2Θ ≤ 50.0°	3.8° ≤ 2Θ ≤ 50.0°	4.6° ≤ 2Θ ≤ 52.0°	4.4° ≤ 2Θ ≤ 50.5°	4.3° ≤ 2Θ ≤ 50.0°
scan speed [° min^{-1}]	ω̇ = 11	ω̇ = 10	ω̇ = 7	ω̇ = 7	ω̇ = 10	ω̇ = 7	ω̇ = 8
no. rflns. measured	4835	3278	5243	10967	3286	6415	3955
no. unique rflns.	4506	3278	4866	10353	3105	6041	3955
no. rflns. observed	3995	3206	3570	8664	2723	3419	2883
observation criterion	$I \geq 2\sigma$	$I \geq 2\sigma$	$I \geq 2\sigma$	$I \geq 2\sigma$	$I \geq 2\sigma$	$I \geq 2\sigma$	$I \geq 2\sigma$
no. param. refined	528	423	314	729	364	431	296
residual el. density [10^{-6} e pm^{-3}]	0.48	0.47	0.64	0.66	1.10	0.76	0.70
R_1 / R_w [%] (refinement on F^2)	3.4 / 8.7	3.0 / 7.1	4.8 / 9.9	3.7 / 10.3	3.9 / 8.6	6.8 / 14.8	3.5 / 8.2

at 0°C. After 10 min., the resulting bright-yellow solution was added to a solution of 20 mmol **1** in 150 ml of THF at 0°C. The reaction was completed by heating to reflux for 2 h, and then quenched by adding 50 ml of water. The phases were separated and the organic phase was dried with $MgSO_4$. The solvent was removed in a rotary evaporator and the product was distilled under reduced pressure through a 15 cm Vigreux column resulting in a light-yellow liquid.

2-Methyl-2-(piperidinomethyl)propane-1,3-diol (**2h**): Yield: 2.82 g (15.1 mmol, 75%), b.p. 110°C (0.8 Torr). – EI-MS; *m/z* (%): 187 (17) [M$^+$], 98 (100) [$CH_2N(CH_2)_5^+$], 84 (37) [$N(CH_2)_5^+$]. – $C_{10}H_{21}NO_2$ (187.28): calcd. C 64.13, H 11.30, N 7.48; found C 63.60, H 11.21, N 7.34.

(±)-2-(Methoxymethyl)-2-(piperidinomethyl)propan-1-ol (**2i**): Yield 1.65 g (8.2 mmol, 41%), b.p. 79°C (0.8 Torr). – EI-MS; *m/z* (%): 201 (42) [M$^+$], 98 (100) [$CH_2N(CH_2)_5^+$]. – $C_{11}H_{23}NO_2$ (201.31): calcd. C 65.63, H 11.52, N 6.96; found C 65.43, H 11.46, N 6.81.

Preparation of **2j**, **2k**, **2l**: 20 mmol of **2** was dissolved in a mixture of 25 ml of water and 25 ml of dioxane. 1.85 g (22 mmol) of $NaHCO_3$ was added and the solution was cooled to 0°C. Then, 4.36 g (20 mmol) of Boc_2O in 20 ml of dioxane was added and the reaction mixture was stirred at room temperature for 12 h. The solvents were then removed at 10^{-1} mbar, the remaining white solid was suspended in Et_2O and filtered through 3 cm of kieselguhr. After evaporation of the solvent from the filtrate, the product remained as a white, microcrystalline solid.

(±)-2-Benzoxymethyl-2-[(tert-butoxycarbonyl)methylaminomethyl]-2-methylpropan-1-ol (**2j**): Yield: 5.32 g (16.5 mmol, 82%). – EI-MS; *m/z* (%): 323 (6) [M$^+$], 176 (50) [M$^+$ – Bn – C_4H_8], 144 (29) [$CH_2NMeBoc^+$], 91 (100) [$C_7H_7^+$]. – $C_{18}H_{29}NO_4$ (323.43): calcd. C 66.84, H 9.04, N 4.33; found C 66.60, H 8.82, N 4.27.

2-[(tert-Butoxycarbonyl)methylaminomethyl]-2-methylpropane-1,3-diol (**2k**): Yield: 4.10 g (17.6 mmol, 88%). – EI-MS; *m/z* (%): 233 (5) [M$^+$], 176 (12) [M$^+$ – C_4H_9], 144 (39) [$CH_2NMeBoc^+$], 129 (38) [$NMeBoc^+$], 88 (13) [M$^+$ – $CH_2NMeBoc$], 56 (100) [$C_4H_8^+$]. – $C_6H_{15}NO_2$ (233.31): calcd. C 56.63, H 9.94, N 6.00; found C 56.67, H 10.06, N 5.90.

2-[Benzyl(tert-butoxycarbonyl)aminomethyl]-2-methylpropane-1,3-diol (**2l**): Yield: 5.58 g (18.1 mmol, 90%). – EI-MS; *m/z* (%): 309 (15) [M$^+$], 253 (22) [M$^+$ – C_4H_9], 218 (35) [M$^+$ – Bn], 164 (31) [M$^+$ – C_4H_9 – Bn], 120 (93) [CH_2NBn^+], 91 (100) [$C_7H_7^+$], 57 (80) [$C_4H_9^+$]. $C_{17}H_{27}NO_4$ (309.41): calcd. C 65.99, H 8.80, N 4.53; found C 66.89, H 8.65, N 4.62.

Reactions Leading to Intramolecular Complications. – 4-(Hydroxymethyl)-4-methyl-2-phenylthiolane (**A**): 4.1 ml of *n*BuLi solution (10.3 mmol of *n*BuLi) in 15 ml of Et_2O was cooled to 0°C. To this solution, 0.85 g (10 mmol) of piperidine was added and the yellow mixture was allowed to warm to room temperature. Then, 830 mg (4 mmol) of **1f** was added dropwise over a period of 5 min. After 2 h, the orange-coloured solution was quenched with 0.2 ml of water. The solvents were removed in a rotary evaporator and the residue was chromatographed on silica gel with a petroleum ether (40–60)/Et_2O mixture: Yield: 0.96 g (3.7 mmol, 92%) of a viscous oil, R_f = 0.37 (PE/Et_2O, 1:1). – ^{1}H NMR ($CDCl_3$): δ = 1.25 (s, 6 H, CqCH_3), 1.81 (br. s, 2 H, O*H*), 1.78–3.22 (m, 8 H, CH_2S, CqCH_2), 3.61, 3.67 (2s, 4 H, CH_2OH), 4.59 (m, 2 H, C*H*Ph) 7.25–7.37 (m, 10 H, arom. *H*). – ^{13}C NMR ($CDCl_3$): δ = 21.4, 22.8 (2s, CqCH_3), 40.9, 41.9 (2s, CH_2Cq), 49.3, 49.4 (2s, *Cq*), 48.8, 49.1, (2s, CH_2S), 50.9, 51.3 (2s, C*H*Ph), 67.6, 69.8 (2s, CH_2OH), 126.9–141.8 (*arom. C*). – EI-MS; *m/z* (%): 209 (100) [M$^+$]. –

$C_{12}H_{16}OS$ (208.31): calcd. C 69.19, H 7.74, S 15.39; found C 69.11, H 7.79, S 15.25.

2-(Diphenylphosphanylmethyl)-2-methylpropan-1-ol (**B**): 0.85 g (10 mmol) of piperidine in 15 ml of toluene was deprotonated with 4.1 ml (10.3 mmol) of *n*BuLi at 0°C. Subsequently, 0.9 g (3 mmol) of **1g** in 10 ml of toluene was added dropwise at room temperature. The yellow reaction mixture was heated to reflux for 20 h, leading to a gradual change in colour from orange to dark-red. The solution was then quenched with 0.2 ml of deoxygenated water and the solvents were removed at 10^{-1} mbar. The residue was chromatographed on silica gel with a petroleum ether (40–60)/Et_2O mixture: Yield: 0.16 g (0.6 mmol, 19%) of a viscous oil, R_f = 0.37 (PE/Et_2O, 2:3). – ^{31}P NMR ($CDCl_3$): δ = –27.0. – ^{1}H NMR ($CDCl_3$): δ = 1.00 (s, 6 H, CqCH_3), 1.50 (br. s, 1 H, O*H*), 2.22 (br. s, 2 H, CH_2P), 3.42 (s, 2 H, CH_2OH), 7.27–7.54 (m, 10 H, arom. *H*).

Tripod Ligands. – Preparation of **3a**, **3b**, **3h**, **3i**: 1 equiv. of the appropriate substituted propane-1,3-diol in THF was deprotonated with 2.2 equiv. of *n*BuLi at 0°C. The resulting yellow solution was allowed to warm to room temperature and subsequently recooled to 0°C. A THF solution of 2.2 equiv. of methanesulfonyl chloride was then added dropwise, and the now colourless reaction mixture was stirred at room temperature for 3 h. In a separate vessel, 2.5 equiv. of diphenylphosphane in THF was deprotonated with 2.75 equiv. of *n*BuLi. The resulting red Li diphenylphosphide solution was slowly added to the reaction mixture at 0°C. After stirring for 10 h at room temperature, the reaction was quenched by the addition of 100 ml of deoxygenated water. The phases were separated and the solvent was evaporated from the organic phase. The resulting pale-yellow oil was chromatographed on silica gel with a petroleum ether (40–60)/Et_2O mixture.

2,2-Bis(diphenylphosphanylmethyl)-N,N-dimethylpropanamine (**3a**): Yield: 16.20 g (33.5 mmol, 67%) of a viscous oil, R_f = 0.31 (PE/Et_2O, 3:1). – EI-MS; *m/z* (%): 483 (30) [M^+], 425 (25) [M^+ – CH_2NMe_2], 406 (86) [M^+ – Ph], 199 (36) [$CH_2PPh_2^+$], 183 (42) [PPh_2^+], 58 (100) [$C_4H_{10}N^+$]. – $C_{31}H_{35}NP_2$ (483.57): calcd. C 77.00, H 7.30, N 2.90, P 12.81; found C 76.73, H 7.70, N 2.39, P 12.69.

2,2-Bis(diphenylphosphanylmethyl)-2-piperidinomethylpropane (**3b**): Yield: 7.33 g (14 mmol, 70%) of a viscous oil, R_f = 0.37 (PE/Et_2O, 9:1). – EI-MS; *m/z* (%): 523 (33) [M^+], 446 (61) [M^+ – Ph], 338 (12) [M^+ – PPh_2], 183 (16) [PPh_2^+], 98 (100) [$CH_2N(CH_2)_5^+$]. – $C_{34}H_{39}NP_2$ (523.64): calcd. C 77.99, H 7.51, N 2.67, P 11.83; found C 77.90, H 7.36, N 2.62, P 11.71.

N-(tert-Butoxycarbonyl)-2,2-bis(diphenylphosphanylmethyl)-N-methylpropanamine (**3h**): Yield: 3.87 g (6.8 mmol, 34%) of a viscous oil, R_f = 0.45 (PE/Et_2O, 3:1). – EI-MS; *m/z* (%): 569 (20) [M^+], 492 (12) [M^+ – Ph], 436 (59) [M^+ – Ph – C_4H_9], 199 (22) [M^+ – 2 PPh_2], 184 (39) [PPh_2^+], 56 (19) [$C_4H_8^+$]. – $C_{35}H_{41}NO_2P_2$ (569.66): calcd. C 73.80, H 7.25, N 2.46; found C 73.60, H 7.66, N 2.34.

N-Benzyl-N-(tert-butoxycarbonyl)-2,2-bis(diphenylphosphanylmethyl)propanamine (**3i**): Yield: 5.87 g (8.5 mmol, 34%) of a viscous oil, R_f = 0.48 (PE/Et_2O, 3:1); EI-MS; *m/z* (%): 645 (20) [M^+], 568 (100) [M^+ – Ph], 512 (50) [M^+ – Ph – C_4H_9], 425 (20) [M^+ – $CH_2NBnBoc$], 183 (36) [PPh_2^+], 91 (47) [$C_7H_7^+$], 57 (22) [$C_4H_9^+$]. – $C_{41}H_{45}NO_2P_2 \cdot 1/2\ Et_2O$ (645.76): calcd. C 75.65, H 7.38, N 2.05, P 9.07; found: C 74.82, H 7.15, N 2.07, P 9.00.

Preparation of **3c**, **3d**: 5 mmol of **3** was dissolved in 10 ml of CH_2Cl_2 and 5 ml of trifluoroacetic acid was added. The solution was stirred for 2 h and then the solvents were removed at 10^{-1} mbar. The resulting highly viscous oil was dissolved in Et_2O and 10 ml of deoxygenated water was added. Residual trifluoroacetic acid was neutralized with KOH (1 N solution in deoxygenated water). The phases were separated and the organic phase was dried with $MgSO_4$. Removal of the solvent at 10^{-1} mbar yielded very viscous oils, which tenaciously retain solvents.

2,2-Bis(diphenylphosphanylmethyl)-N-methylpropanamine (**3c**): Yield: 2.31 g (4.9 mmol, 99%). – EI-MS; *m/z* (%): 469 (21) [M^+], 425 (12) [M^+ – CH_2NCH_3], 392 (100) [M^+ – Ph], 199 (22) [$CH_2PPh_2^+$], 183 (39) [PPh_2^+], 84 (53) [$C_5H_{10}N^+$]. – $C_{30}H_{33}NP_2 \cdot 1/6\ CH_2Cl_2$ (469.55): calcd. C 74.91, H 6.95, N 2.90, P 12.81; found C 75.27, H 6.99, N 2.91, P 12.73.

N-Benzyl-2,2-bis(diphenylphosphanylmethyl)propanamine (**3d**): Yield: 2.67 g (4.9 mmol, 97%). – EI-MS; *m/z* (%): 545 (4) [M^+], 470 (20) [M^+ – Ph], 254 (47) [M^+ – NHBn – PPh_2], 199 (39) [$CH_2PPh_2^+$], 185 (36) [PPh_2^+], 160 (37) [M^+ – CH_2PPh_2 – PPh_2], 91 (100) [$C_7H_7^+$]. – $C_{36}H_{37}NP_2 \cdot 1/2\ Et_2O$ (545.64): calcd. C 78.22, H 7.01, N 2.47, P 10.90; found C 78.56, H 7.09, N 2.47, P 10.98.

Preparation of **3e**, **3f**: The preparations of **3e** and **3f** were carried out similarly to that of **3a**. Half of the stated amounts of *n*BuLi (deprotonation of the alcohol moiety), methanesulfonyl chloride, and Li phosphide were employed.

(±)-2-(Diphenylphosphanylmethyl)-2-(isopropylsulfanylmethyl)-N,N-dimethylpropanamine (**3e**): Yield: 7.88 g (21.1 mmol, 84%) of a viscous oil, R_f = 0.28 (PE/Et_2O, 9:1). – EI-MS; *m/z* (%): 374 (25) [M^+], 330 (68) [M^+ – NMe_2], 183 (33) [PPh_2^+], 58 (100) [$C_4H_{10}N^+$]. – $C_{22}H_{32}NPS$ (373.54): calcd. C 70.74, H 8.63, N 3.75, P 8.29, S 8.58; found C 70.28, H 8.74, N 3.63, P 8.17, S 8.66.

(±)-2-(Benzylsulfanylmethyl)-2-(diphenylphosphanylmethyl)-N,N-dimethylpropanamine (**3f**): Yield: 4.78 g (11.3 mmol, 77%) of a viscous oil, R_f = 0.38 (PE/Et_2O, 3:1). – EI-MS; *m/z* (%): 422 (50) [M^+], 330 (68) [M^+ – NMe_2], 183 (33) [PPh_2^+], 58 (100) [$C_4H_{10}N^+$]. – $C_{26}H_{32}NPS$ (421.58): calcd. C 74.08, H 7.65, N 3.32, P 7.35, S 7.60; found C 74.02, H 7.81, N 3.35, P 7.52, S 7.20.

Preparation of **3g**: The reductive cleavage of the SBn bond in **3f** was achieved with Li/NH_3/THF following a published procedure[9].

(±)-2-(Diphenylphosphanylmethyl)-2-(sulfanylmethyl)-N,N-dimethylpropanamine (**3g**): Yield: 1.43 g (4.3 mmol, 78%) of a viscous oil, R_f = 0.35 (PE/Et_2O, 1:1). – EI-MS; *m/z* (%): 330 (4) [M^+], 298 (15) [M^+ – SH], 199 (22) [$CH_2PPh_2^+$], 183 (28) [PPh_2^+], 58 (100) [$C_4H_{10}N^+$]. – $C_{19}H_{26}NPS$ (331.46): calcd. C 68.85, H 7.91, N 4.23; found C 68.52, H 7.93, N 4.18.

Coordination Chemistry

Tetracarbonyl Molybdenum Compounds. – Preparation of **4a**–**4e**: 1 mmol of **3** was dissolved in 100 ml of freshly distilled toluene. 264 mg (1 mmol) of $Mo(CO)_6$ was added and the mixture was heated to reflux for 4 h. The toluene was then removed at 10^{-1} mbar. The resulting brown solid was washed three times with petroleum ether (40–60) to remove excess $Mo(CO)_6$. Crystals suitable for X-ray structural analysis were obtained by vapour diffusion of petroleum ether (40–60) into a solution of the crude product in CH_2Cl_2 (**4a**, **4d**, **4e**).

{η²-P,P-[2,2-Bis(diphenylphosphanylmethyl)-N,N-dimethylpropanamine]}tetracarbonylmolybdenum(0) (**4a**): Yield: 486 mg (0.7 mmol, 70%) of a brown solid. Recrystallization afforded 346 mg (0.5 mmol, 50%) of yellow crystals, m.p. 104–106°C. – $C_{35}H_{35}MoNO_4P_2$ (691.55): calcd. C 60.79, H 5.10, N 2.03; found C 60.45, H 5.16, N 1.84.

{η²-P,P-[2,2-Bis(diphenylphosphanylmethyl)-2-(piperidinomethyl)propane]}tetracarbonylmolybdenum(0) (**4b**): Yield: 586 mg (0.8 mmol, 81%) of a brown solid. Recrystallization afforded 244

mg (0.3 mmol, 34%) of yellow crystals, m.p. 103–107°C. – $C_{38}H_{29}MoNO_4P_2$ (721.54): calcd. C 63.26, H 4.05, N 1.94; found C 61.79, H 5.42, N 1.84.

{η²-P,P-[2,2-Bis(diphenylphosphanylmethyl)-N-methylpropanamine]}tetracarbonylmolybdenum(0) (**4c**): Yield: 600 mg (0.9 mmol, 89%) of a brown solid, m.p. 104°C. – $C_{34}H_{33}MoNO_4P_2$ (677.53): calcd. C 60.27, H 4.91, N 2.07; found C 57.24, H 4.83, N 1.95.

{η²-P,P-[N-Benzyl-2,2-bis(diphenylphosphanylmethyl)-propanamine]}tetracarbonylmolybdenum(0) (**4d**): Yield: 522 mg (0.7 mmol, 69%) of a brown solid, m.p. 115°C. – $C_{40}H_{37}MoNO_4P_2$ (753.63): calcd. C 63.75, H 4.95, N 1.86; found C 61.97, H 5.20, N 1.76.

{η²-P,S-[2-(Diphenylphosphanylmethyl)-2-(isopropylsulfanylmethyl)-N,N-dimethylpropanamine]}tetracarbonylmolybdenum(0) (**4e**): Recrystallization of the crude product afforded 187 mg (0.3 mmol, 32%) of yellow crystals, m.p. 125–130°C. – $C_{26}H_{32}MoNO_4PS$ (581.52): calcd. C 53.70, H 5.55, N 2.41, P 5.33; found C 52.28, H 5.87, N 2.18, P 5.06.

{η²-P,S-[2-(Benzylsulfanylmethyl)-2-(diphenylphosphanylphosphanylmethyl)-N,N-dimethylpropanamine]}tetracrbonylmolybdenum(0) (**4f**): The preparation of **4f** was carried out similarly to that described for **4a**. However, excess $Mo(CO)_6$ could not be removed by washing with petroleum ether (40–60) since **4f** is freely soluble in this solvent. Recrystallization of the crude product from petroleum ether (40–60) afforded 249 mg (0.4 mmol, 39%) of yellow crystals, m.p. 134–137°C. – $C_{30}H_{32}MoNO_4PS$ (629.56): calcd. C 57.24, H 5.12, N 2.22, P 4.92, S 5.09; found C 56.20, H 5.30, N 2.15, P 4.85, S 5.05.

Tricarbonyl Molybdenum Compounds. – Preparation of **5a**, **5b**: A stirred solution of 1 mmol of **3** in 100 ml of CH_2Cl_2 was cooled to –70°C and 0.95 mmol (288 mg) of freshly prepared $(CH_3CN)_3Mo(CO)_3$ was added. After 2–4 h, all of the $(CH_3CN)_3Mo(CO)_3$ had dissolved, resulting in a clear yellow solution. The solvent was then removed at 10^{-1} mbar without heating the solution. The products were recrystallized by vapour diffusion of petroleum ether (40–60) into a solution of **5** in CH_2Cl_2 at 0°C.

(±)-[2,2-Bis(diphenylphosphanylmethyl)-N-methylpropanamine]tricarbonylmolybdenum(0) (**5a**): Yield: 586 mg (0.8 mmol, 81%) of a yellow solid. Recrystallization afforded 298 mg (0.5 mmol, 46%) of yellow crystals, m.p. 168–174°C (dec). – $C_{33}H_{33}MoNO_3P_2$ (649.52): calcd. C 61.02, H 5.12, N 2.16, P 9.54; found C 60.53, H 5.41, N 2.07, P 9.46.

(±)-[N-Benzyl-2,2-bis(diphenylphosphanylmethyl)-propanamine]tricarbonylmolybdenum(0) (**5b**): Yield: 548 mg (0.8 mmol, 75%) of a yellow solid. Recrystallization afforded 197 mg (0.3 mmol, 27%) of yellow crystals, m.p. 200–205°C (dec). – $C_{39}H_{37}MoNO_3P_2$ (725.62): calcd. C 64.56, H 5.14, N 1.93, P 8.54; – found C 62.77, H 5.17, N 1.87, P 8.45.

[2-(Diphenylphosphanylmethyl)-2-(isopropylsulfanylmethyl)-N,N-dimethylpropanamine]tricarbonylmolybdenum(0) (**5c**): The preparation of **5c** was carried out similarly to that described for **5a** (see above). After 3 h, the clear yellow reaction solution was concentrated to half of the initial volume and layered with petroleum ether (40–60). After two days at 0°C, 174 mg (0.3 mmol, 31%) of long, yellow needles suitable for X-ray structural analysis were obtained; m.p. 145–147°C (dec). – $C_{25}H_{32}MoNO_3PS$ (553.51): calcd. C 54.25, H 5.83, N 2.53, P 5.60, S 5.79; found C 53.69, H 6.02, N 2.43, P 5.59, S 5.64.

Interconversion of $Mo(CO)_3$ and $Mo(CO)_4$ Derivatives. – Conversion of **5c** *to* **4e**: 0.61g (1.1 mmol) of **5c** was dissolved in 100 ml of CH_2Cl_2. The solution was stirred while CO (1 bar) was bubbled through it. After 1h, only the ν_{CO} IR band pattern of a tetracarbonyl species could be detected. The solvent was removed at 10 $^{-1}$ mbar affording 0.61 g (1 mmol, 95%) of a dark-yellow solid, which showed ^{31}P-NMR, IR, and mass spectra identical to those of **4e**.

Conversion of **4e** *to* **5c**: 0.75 g (1.3 mmol) of **4e** was dissolved in 100 ml of THF. The solution was irradiated at –5°C in a 2-propanol-cooled Duran-50 glass apparatus with a mercury lamp (TQ 150 Hanau). IR-samples were taken periodically to monitor the progress of the reaction. After 12 h, only the ν_{CO} IR band pattern of a tricarbonyl species was detectable. The solvent was removed at 10^{-1} mbar resulting in 0.6 g (1.1 mmol, 85%) of a brown solid showing ^{31}P-NMR, IR, and mass spectra identical to those of **5c**.

[1] See for example: [1a] T. G. Gardner, G. S. Girolami, *Organometallics* **1987**, *6*, 2551. – [1b] C. Bianchini, C. Ghilardi, A. Meli, S. Midollini, A. Orlandini, *J. Organomet. Chem.* **1983**, *248*, C13. – [1c] C. Bianchini, A. Meli, A. Orlandini, L. Sacconi, *J. Organomet. Chem.* **1981**, *218*, 81. – [1d] C. Bianchini, C. Mealli, A. Meli, A. Orlandini, *Inorg. Chem.* **1980**, *19*, 2968.

[2] [2a] L. Sacconi, F. Mani, *Transition Met. Chem.* **1982**, *8*, 179 and references cited therein. – [2b] S. Friedrich, H. Memmler, L. H. Gade, W.-S. Li, M. McPartlin, *Angew. Chem.* **1994**, *106*, 705; *Angew Chem., Int. Ed. Engl.* **1994**, *33*, 676. – [2c] A. Barth, G. Huttner, M. Fritz, L. Zsolnai, *Angew. Chem.* **1990**, *102*, 956; *Angew. Chem., Int. Ed. Engl.* **1990**, *29*, 929. – [2d] P. Barbaro, C. Bianchini, P. Frediani, A. Meli, F. Vizza, *Inorg. Chem.* **1992**, *31*, 1523.

[3] [3a] S. Beyreuther, J. Hunger, G. Huttner, S. Mann, L. Zsolnai, *Chem. Ber.* **1996**, *129*, 745. – [3b] J. Hunger, S. Beyreuther, G. Huttner, *J. Mol. Model.* **1996**, *2*, 257. – [3c] S. Beyreuther, J. Hunger, G. Huttner, *J. Mol. Model.* **1996**, *2*, 273.

[4] [4a] C. Bianchini, A. Meli, M. Peruzzini, F. Vizza, *Organometallics* **1990**, *9*, 226. – [4b] E. G. Thaler, K. Folting, K. G. Caulton, *J. Am. Chem. Soc.* **1990**, *112*, 2664. – [4c] M. J. Burk, J. E. Feaster, R. L. Harlow, *Tetrahedron: Asymmetry* **1991**, *2*, 569. – [4d] V. Sernau, G. Huttner, M. Fritz, L. Zsolnai, O. Walter, *J. Organomet. Chem.* **1993**, *453*, C23. – [4e] J. Scherer, G. Huttner, H. Heidel, *J. Organomet. Chem.*, accepted.

[5] [5a] S.-T. Liu, G.-J. Liu, C.-H. Yieh, M.-C. Cheng, S.-M. Peng, *J. Organomet. Chem.* **1990**, *387*, 83. – [5b] S.-T. Liu, H.-E. Wang, M.-C. Cheng, S.-M. Peng, *J. Organomet. Chem.* **1989**, *376*, 333. – [5c] S.-T. Liu, K.-J. Liu, *Inorg. Chem.* **1990**, *29*, 4576. – [5d] S.-T. Liu, C.-H. Yieh, H.-J. Lu, *Phosphorus, Sulfur and Silicon* **1989**, *44*, 261. – [5e] S.-T. Liu, C.-L. Tsao, M.-C. Cheng, S.-M. Peng, *Polyhedron* **1990**, *9*, 2579. – [5f] S.-T. Liu, *J. Chin. Chem. Soc.* **1992**, *39*, 611. – [5g] S.-C. Tsai, H.-E. Wang, S.-T. Wang, L.-M. Yiin, S.-T. Liu, *Chem. Ber.* **1995**, *128*, 151. – [5h] T. Seitz, A. Muth, G. Huttner, *Chem. Ber.* **1994**, *127*, 1837. – [5i] T. Seitz, A. Muth, G. Huttner, *Z. Naturforsch.* **1995**, *50b*, 1045. – [5j] O. Walter, T. Klein, G. Huttner, L. Zsolnai, *J. Organomet. Chem.* **1993**, *458*, 63. – [5k] A. Muth, G. Reinhard, G. Huttner, T. Seitz, T. Klein, L. Zsolnai, *Z. Naturforsch.* **1994**, *49b*, 889. – [5l] G. Reinhard, R. Soltek, G. Huttner, A. Barth, O. Walter, *Chem. Ber.* **1996**, *129*, 97. – [5m] J. Scherer, G. Huttner, M. Büchner, J. Bakos, *J. Organomet. Chem.* **1996**, *520*, 45. – [5n] J. Scherer, G. Huttner, M. Büchner, *Chem. Ber.* **1996**, *129*, 697.

[6] [6a] H. Heidel, G. Huttner, G. Helmchen, *Z. Naturforsch.* **1993**, *48b*, 1681. – [6b] H. Heidel, G. Huttner, R. Vogel, G. Helmchen, *Chem. Ber.* **1994**, *127*, 271. – [6c] H. Heidel, G. Huttner, L. Zsolnai, *Z. Naturforsch.* **1995**, *50b*, 729.

[7] [7a] I. Dostrovsky, E. D. Hughes, C. K. Ingold, *J. Chem. Soc.* **1946**, 173. – [7b] D. Cook, A. J. Parker, *J. Chem. Soc. B* **1968**, 142. – [7c] M. H. Abraham, P. L. Grellier, M. J. Hogarth, *J. Chem. Soc., Perkin Trans. 2* **1975**, 1365

[8] [8a] H.-E. Wang, C.-Y. Liu, M.-C. Cheng, S.-M. Peng, S.-T. Liu, *Phosphorus, Sulfur and Silicon* **1992**, *69*, 201. – [8b] S.-T. Liu, C.-Y. Liu, *J. Org. Chem.* **1992**, *57*, 6079. – [8c] S.-T. Liu, C.-H. Yieh, H.-P. Dai, *Proc. Natl. Sci. Counc. (A)* **1995**, *19*, 1.

[9] R. Soltek, G. Huttner, L. Zsolnai, A. Driess, *Inorg. Chim. Acta*, submitted.

[10] H. Stetter, W. Boeckmann, *Chem. Ber.* **1951**, *84*, 834.

[11] H. Reiff, D. Dieterich, R. Braden, H. Ziemann, *Liebigs Ann. Chem.* **1973**, 365.
[12] [12a] D. B. Pattison, *J. Am. Chem. Soc.* **1957**, *75*, 3455. – [12b] J. Cheymol, P. Chabrier, J. Seyden-Penne, A. Habert-Somny, T. Strazalko, *Bull. Soc. Chim. Fr.* **1965**, 694. – [12c] A. J. McAlees, R. McCrindle, A. R. Woon-Fat, *Inorg. Chem.* **1976**, *15*, 1065. – [12d] M. Motoi, H. Suda, S. Katsuhiko, S. Nagahara, M. Takei, K. Shigeyoshi, *Bull. Chem. Soc. Jpn.* **1988**, *61*, 1653.
[13] S. Searles, V. P. Gregory, *J. Am. Chem. Soc.* **1954**, *76*, 2789.
[14] C. Calderoni, V. Cere, S. Pollicino, E. Sandri, A. Fava, *J. Org. Chem.* **1980**, *45*, 2641.
[15] P. J. Kocienski "Protecting groups", *Thieme Foundation of Organic Chemistry* series, Thieme, Stuttgart, New York, **1994**.
[16] D. P. Tate, W. R. Knipple, J. M. Augl, *Inorg. Chem.* **1962**, *1*, 433.
[17] Tables of the fractional atomic coordinates are available from the author on request. Further details of the crystal structure investigations may be obtained from the Fachinformationszentrum Karlsruhe, D-76344 Eggenstein-Leopoldshafen (Germany), on quoting the depository numbers CSD-406954 (**4a**), CSD-406958 (**4b**), CSD-406956 (**4e**), CSD-406960 (**4f**), CSD-406957 (**5a**), CSD-406959 (**5b**), CSD-406955 (**5c**).
[18] The IUPAC 1974 Recommendations, Section E, *Pure Appl. Chem.* **1976**, *45*, 13.
[19] *Organikum*, Deutscher Verlag der Wissenschaften, Berlin **1990**, 638.
[20] [20a] G.M.Sheldrick, *SHELXS-86*, University of Göttingen **1986**. – [20b] G.M.Sheldrick, *SHELX-93*, University of Göttingen **1993**. – [20c] *International Tables for X-ray Crystallography, vol. 4*, Kynoch Press, Birmingham, **1974**.
[21] L. Zsolnai, G. Huttner, *XPMA*, University of Heidelberg, **1994**.
[97114]